JGP Journal of General Physiology

ARTICLE

Prostaglandin E_2 stimulates the epithelial sodium channel (ENaC) in cultured mouse cortical collecting duct cells in an autocrine manner

Morag K. Mansley[1*], Christian Niklas[1*], Regina Nacken[1], Kathrin Mandery[2], Hartmut Glaeser[2], Martin F. Fromm[2], Christoph Korbmacher[1], and Marko Bertog[1]

Prostaglandin E_2 (PGE_2) is the most abundant prostanoid in the kidney, affecting a wide range of renal functions. Conflicting data have been reported regarding the effects of PGE_2 on tubular water and ion transport. The amiloride-sensitive epithelial sodium channel (ENaC) is rate limiting for transepithelial sodium transport in the aldosterone-sensitive distal nephron. The aim of the present study was to explore a potential role of PGE_2 in regulating ENaC in cortical collecting duct (CCD) cells. Short-circuit current (I_{SC}) measurements were performed using the murine $mCCD_{cl1}$ cell line known to express characteristic properties of CCD principal cells and to be responsive to physiological concentrations of aldosterone and vasopressin. PGE_2 stimulated amiloride-sensitive I_{SC} via basolateral prostaglandin E receptors type 4 (EP_4) with an EC_{50} of ∼7.1 nM. The rapid stimulatory effect of PGE_2 on I_{SC} resembled that of vasopressin. A maximum response was reached within minutes, coinciding with an increased abundance of β-ENaC at the apical plasma membrane and elevated cytosolic cAMP levels. The effects of PGE_2 and vasopressin were nonadditive, indicating similar signaling cascades. Exposing $mCCD_{cl1}$ cells to aldosterone caused a much slower (∼2 h) increase of the amiloride-sensitive I_{SC}. Interestingly, the rapid effect of PGE_2 was preserved even after aldosterone stimulation. Furthermore, application of arachidonic acid also increased the amiloride-sensitive I_{SC} involving basolateral EP_4 receptors. Exposure to arachidonic acid resulted in elevated PGE_2 in the basolateral medium in a cyclooxygenase 1 (COX-1)–dependent manner. These data suggest that in the cortical collecting duct, locally produced and secreted PGE_2 can stimulate ENaC-mediated transepithelial sodium transport.

Introduction

In the kidney the amiloride-sensitive epithelial sodium channel (ENaC) is localized to the apical membrane of tubular epithelial cells lining the so-called aldosterone-sensitive distal nephron (ASDN). This comprises the late distal convoluted tubule, the connecting tubule, and the collecting duct (CD). In the ASDN, transepithelial sodium transport critically depends on the activity and abundance of ENaC. The precise regulation of ENaC is essential for the fine-tuning of urinary sodium excretion to match dietary sodium intake. Thus, ENaC regulation plays a key role for total body sodium balance and is critical for the long-term control of extracellular fluid volume and arterial blood pressure. ENaC is regulated by several hormones, including aldosterone and vasopressin, as well as by several local factors (Garty and Palmer, 1997; Loffing and Korbmacher, 2009; Bankir et al., 2010; Rossier, 2014; Kleyman et al., 2018).

Prostanoids are derivatives of arachidonic acid and are produced and secreted by many different cells. Prostanoids have complex effects on renal function (Grantham and Orloff, 1968; Breyer and Breyer, 2000b) and contribute to the regulation of sodium and water excretion, renin secretion, renal blood flow, and glomerular filtration (Hao and Breyer, 2007). Because they are rapidly metabolized, these derivatives are thought to act within close proximity to the site of their synthesis in either an autocrine or paracrine manner (Fenton and Knepper, 2007). Prostaglandin E_2 (PGE_2), derived via cyclooxygenase (COX), is the most abundant prostanoid in the kidney. There are conflicting reports regarding the effects of PGE_2 on sodium and water transport within the collecting duct (Breyer and Breyer 2000a). Several studies suggest that in the renal medulla, PGE_2 reduces sodium absorption (Stokes and Kokko, 1977; Iino and Imai, 1978). In contrast, inhibition of prostaglandin synthesis has been reported to be associated with increased urinary sodium excretion in conscious dogs, probably due to diminished

[1]Institute of Cellular and Molecular Physiology, Friedrich-Alexander University Erlangen-Nürnberg, Erlangen, Germany; [2]Institute of Experimental and Clinical Pharmacology and Toxicology, Friedrich-Alexander University Erlangen-Nürnberg, Erlangen, Germany.

*M.K. Mansley and C. Niklas contributed equally to this paper; Correspondence to Christoph Korbmacher: christoph.korbmacher@fau.de; Marko Bertog: marko.bertog@fau.de.

sodium reabsorption in the collecting duct (Kirschenbaum and Stein, 1976). Moreover, PGE_2 may be able to stimulate water and sodium absorption within the cortical CD (CCD) to maintain blood pressure in volume-contracted states (Hao and Breyer, 2008).

PGE_2 exerts its diverse effects by binding to four distinct G protein–coupled receptors: EP_1–EP_4 (Hao and Breyer, 2007). The expression pattern of these receptors determines local effects of PGE_2 (Breyer and Breyer, 2000b). EP_2 and EP_4 receptors are $G_{\alpha s}$-coupled receptors, and ligand binding to these receptors stimulates adenylyl cyclase (AC), raising cytosolic cAMP concentration. In addition, alternative EP_4 receptor pathways may play a role in mediating downstream effects (Fujino and Regan, 2006; Li et al., 2017). EP_3 receptor is coupled to $G_{\alpha i/o}$ and has an inhibitory effect on AC, thereby lowering cytosolic cAMP concentration. The EP_1 receptor is $G_{\alpha q/11}$ coupled and promotes signaling via inositol 1,4,5-trisphosphate (IP_3) and diacylglycerol resulting in elevated intracellular Ca^{2+} concentration and activation of protein kinase C (PKC; Narumiya et al., 1999; Breyer and Breyer, 2001).

Findings in animal models of nephrogenic diabetes insipidus indicate a likely role of prostaglandins in regulating renal water transport. In these animals EP_2 and EP_4 receptor activation alleviated urine-concentrating defects (Li et al., 2009; Olesen et al., 2011). Conversely, nephron-specific or collecting duct-specific knockout of EP_4 receptor in mice promoted urine-concentrating defects (Gao et al., 2015). Interestingly, in in vitro studies of the collecting duct activation of EP_2 and EP_4 receptors promoted apical targeting and phosphorylation of aquaporin-2 water channels, reminiscent of the effect of vasopressin (Olesen et al., 2011, 2016; Gao et al., 2015). Vasopressin-dependent coupling between amiloride-sensitive sodium transport and water flow has been demonstrated in a mouse CCD cell line ($mCCD_{cl1}$; Gaeggeler et al., 2011) as well as in isolated perfused rat CCDs (Reif et al., 1986). Presently, it is not known whether a potential modulatory effect of PGE_2 on tubular water transport is associated with an effect of PGE_2 on ENaC-mediated sodium absorption in the CCD.

The aim of the present study was to investigate whether PGE_2 modifies ENaC-mediated transepithelial sodium transport in $mCCD_{cl1}$ cells. This cell line provides a highly differentiated and hormone-responsive model of CCD principal cells (Gaeggeler et al., 2005, 2011). It is well suited to study the regulation of electrogenic transepithelial ion transport by hormonal and local mediators (Edinger et al., 2014; Mansley et al., 2015, 2018, 2019). We sought to identify the prostaglandin receptors present in this model and explored the interplay between PGE_2 and two key hormones that promote salt and water reabsorption in the CCD, namely aldosterone and vasopressin. Finally, we investigated whether PGE_2 is synthesized and secreted by $mCCD_{cl1}$ cells.

Materials and methods

Cell culture

Mouse CCD cells ($mCCD_{cl1}$) were kindly provided by Bernard Rossier (University of Lausanne, Lausanne, Switzerland) and cultured as described previously (Gaeggeler et al., 2005; Mansley et al., 2015, 2018). Cells were routinely passaged every 7 d (passage 25–34) and maintained in cell culture dishes at 37°C in a 5% CO_2 atmosphere in Dulbecco's modified Eagle's Medium (DMEM)/Ham's F12 (1:1 vol/vol) medium supplemented with 2% FBS, 1 nM triiodothyronine, 60 nM sodium selenite, 10 ng·ml^{-1} epidermal growth factor, 5 µg·ml^{-1} human apotransferrin, 50 nM dexamethasone, 5 µg·ml^{-1} insulin, 100 U·ml^{-1} penicillin, and 100 µg·ml^{-1} streptomycin. For experimental procedures, cells were seeded onto Millicell-PCF culture plate inserts (EMD Millipore) with a membrane pore size of 0.4 µm and an effective surface area of either 0.6 cm^2 or 4.2 cm^2 and grown to form a polarized epithelial monolayer. At day 5 after seeding, the cell culture medium was replaced by a medium devoid of FBS, apotransferrin, and epidermal growth factor. Finally, 24 h before experiments, dexamethasone was removed from the medium.

Chemicals and solutions

DMEM/Ham's F12 (1:1 vol/vol) without phenol red was from Life Technologies and FBS from PAA and Bio&Sell. SC-560, AH23848, AH6809, GW627368X, and Sulprostone were from Cayman Chemical (Biozol); PGE_2 and indomethacin were from Enzo Life Sciences. TCS2510 was from Tocris. Lumiracoxib was kindly provided by Prof. Dr. K. Brune (Institute of Experimental and Clinical Pharmacology and Toxicology, Friedrich-Alexander University, Erlangen, Germany). All other drugs were ordered from Sigma-Aldrich.

Transepithelial measurements

Experimental procedures were essentially the same as described previously (Bertog et al., 2008; Mansley et al., 2015, 2018). Briefly, transepithelial voltage (V_{te}) and resistance (R_{te}) were routinely checked using a commercially available epithelial volt-ohm meter and a set of two sticks "STX" electrodes (World Precision Instruments). On days 9–11, inserts with confluent $mCCD_{cl1}$ cell monolayers were transferred to Ussing chambers for continuous equivalent short-circuit current (I_{SC}) measurements using a CVC6 clamp device (Fiebig) as described previously (Bertog et al., 1999). Alternatively, modified Ussing chambers were used and kept in an incubator gassed with 5% CO_2, and the temperature was maintained at 37°C (Mansley et al., 2015, 2018). These miniaturized chambers were designed to minimize mechanical perturbations and to reduce the bath volumes in the apical and basolateral compartment to 0.35–0.6 ml and 0.55–1.0 ml, respectively. Both experimental approaches showed similar results in the transepithelial parameters investigated. R_{te} was evaluated every 2–30 s by measuring voltage deflections induced by 400-ms symmetrical square current pulses of ± 3–5 µA. Using R_{te} and open-circuit V_{te}, the equivalent I_{SC} was calculated according to Ohm's law. Conventionally, a lumen-negative V_{te} corresponds to a positive I_{SC} which may be due to electrogenic cation absorption, electrogenic anion secretion or a combination of both. After transfer into Ussing chambers, cells were allowed to equilibrate for 30 to 60 min before manipulations took place. At the end of each experiment, amiloride (10 µM) was applied to the apical compartment to determine the ENaC-mediated I_{SC} component.

Reverse transcription (RT) PCR

Total RNA was extracted from $mCCD_{cl1}$ cells following transepithelial measurements using NucleoSpin RNA Kit-XS (Macherey-Nagel)

Table 1. **Primer pairs of target genes used for RT-PCR in this study**

cDNA	Sense primer (5′→3′)	Antisense primer (5′→3′)
EP_1	CGCAGGGTTCACGCACACGA	CACTGTGCCGGGAACTACGC
EP_2	AGGACTTCGATGGCAGAGGAG AC	CAGCCCCTTACACTTCTCCAATG
EP_3	CCGGGCACGTGGTGCTTCAT	TAGCAGCAGATAAACCCAGG
EP_4	TTCCGCTCGTGGTGCGAGTGT TC	GAGGTGGTGTCTGCTTGGGTCAG
COX-1	CCTCTTTCCAGGAGCTCACA	CGGGTAGAACTCTAAAGCATCG
COX-2	GGGAGTCTGGAACATTGTGAA	GCACATTGTAAGTAGGTGGAC TGT
mPGES1	AGCACACTGCTGGTCATCAA	CTCCACATCTGGGTCACTCC
mPGES2	GACCCTGTACCAGTACAAGAC	GAGGAGTCATTGAGCTGTTGC
cPGES	CGAATTTTGACCGTTTCTCTG	TGAATCATCATCTGCTCCATCT
β-Actin	TCACCCACACTGTGCCCATCT AC	GAGTACTTGCGCTCAGGAGGAGC

according to the manufacturer's instructions. Lysates from two 0.6-cm^2 cell culture plate inserts were pooled to enhance the RNA concentration.

For prostanoid receptors (EP_1–EP_4), RT and PCR amplification were performed using an RNA Reverse Transcription System Kit (Promega). Specific primers (Table 1) for murine EP_1–EP_4 receptors and β-actin were designed as described previously (Arakawa et al., 1996) and synthesized by Invitrogen. PCR cycling conditions were 95°C for 2 min, followed by 32 repeats of 95°C for 30 s, 60°C for 45 s, and 72°C for 1 min. Final extension time was 4 min at 72°C.

For all other primers, RT was performed with 0.5 µg RNA using QuantiTect Reverse Transcription Kit (Qiagen) as per the manufacturer's protocol. Specific primers for the COX isoenzymes 1 and 2 (COX-1 and COX-2) and for the cytosolic PGE_2 synthase (cPGES) were designed using universal probe library system (Roche), whereas specific primers for the microsomal PGE synthases-1 and -2 (mPGES1 and, mPGES2) were designed as described previously (mPGES1: Soodvilai et al., 2009; mPGES2: Yang et al., 2006a). Primers were obtained from biomers.net. PCR was performed using 10 pM specific primers in PCR buffer (buffer Y; Peqlab). Samples were denatured for 5 min at 95°C, followed by 35 repeats of 94°C for 1 min, 60°C for 1 min, and 72°C for 1 min. Final extension time was 10 min at 72°C. All reactions were performed in a MJ-Research PTC-200 Peltier Thermo Cycler (Biozym). Amplified PCR products were separated by agarose gel electrophoresis (1.5% universal agarose; Bio&Sell) and stained by ethidium bromide. Bands of PCR products were extracted and sequenced (LGC Genomics). For sequence comparison we used the standard nucleotide BLAST software (National Center for Biotechnology Information, National Library of Medicine).

Biotinylation assay and Western blotting

To detect β-ENaC in Western blot experiments, a previously described custom-made antibody was used in a 1:2,000 dilution (Krueger et al., 2009; Nesterov et al., 2016; Mansley et al., 2018). Horseradish peroxidase–coupled goat anti-rabbit antibodies were obtained from Santa Cruz Biotech and used in a dilution of 1:50,000.

Cell surface proteins were labeled using a biotinylation protocol similar to that previously described for surface biotinylation of lung epithelial cell monolayers (Woollhead and Baines, 2006). For biotinylation experiments, $mCCD_{cl1}$ cells were grown on permeable supports (Millicell-PCF inserts, membrane size 4.2 cm^2; EMD Millipore) for 10 d. All biotinylation steps were performed at 4°C. Cells were chilled to 4°C by washing three times with ice-cold PBS containing 0.7 mM $MgCl_2$ and 0.5 mM $CaCl_2$ (PBS-CM). Cells were kept on ice, and biotinylation of the apical cell surface was achieved by adding borate buffer containing 85 mM NaCl, 5 mM KCl, and 15 mM $Na_2B_4O_7$, pH 9.0, containing 0.5 mg·ml^{-1} EZ-link sulfo-NHS-SS-Biotin (Pierce). The basolateral compartment was exposed to PBS-CM + 10% FBS. Cells were kept on ice and rocked for 30 min. Cells were washed once with PBS-CM and then the reaction quenched by exposing both the apical and basolateral surface of cells to PBS-CM + 10% FBS for a further 30 min. Cells were washed twice with PBS-CM and then scraped into 200 µl lysis buffer (0.4% deoxycholic acid, 1% Triton X-100, 50 mM EGTA, and 10 mM Tris, pH 7.4) including a protease inhibitor cocktail (Roche). A small sample was taken to determine protein content by BCA assay. Biotinylated proteins were captured by exposing the sample to 50 µl ImmunoPure immobilized Neutravidin agarose beads (Pierce), which had been washed twice with PBS-CM and subsequently with lysis buffer. 250 µg sample was added to the washed beads, and tubes were incubated on a rotor overnight at 4°C. Samples were centrifuged for 2 min at 8,000 rpm (6,200 ×*g*) at 4°C, and the supernatant was collected separately for the detection of intracellular proteins. Neutravidin beads were washed and centrifuged four times and the biotinylated fraction was finally resuspended in 45 µl of 2× reducing SDS-PAGE sample buffer (Rotiload 1; Roth).

All protein samples were heated for 5 min at 95°C before loading on SDS gels. Proteins were separated by 10% SDS-PAGE, transferred to polyvinylidene diflouride membranes by semidry electroblotting, and probed with the indicated antibodies. Chemiluminescent signals were detected using Super Signal West Femto Chemiluminescent Substrate (Pierce).

Measurement of PGE_2 and cAMP concentrations

For PGE_2 measurements, an enzyme immunoassay was used according to the manufacturer's protocol (Prostaglandin E_2 Express EIA Kit—Monoclonal; Cayman Chemical Company). PGE_2 concentrations were determined in diluted basolateral cell culture medium after incubating $mCCD_{cl1}$ cells with arachidonic acid, COX inhibitors, or vehicle at 37°C for 10 min.

For cAMP measurements, $mCCD_{cl1}$ cells were lysed to release intracellular cAMP, which was quantified using an enzyme immunoassay according to the manufacturer's instructions (cAMP Biotrak competitive enzyme immunoassay system; GE Healthcare). Cytosolic cAMP concentrations were determined in cells exposed to PGE_2 or vehicle at 37°C for 10 min. Protein concentrations were determined with a bicinchoninic acid assay (BCA Protein Assay Kit; Thermo Scientific).

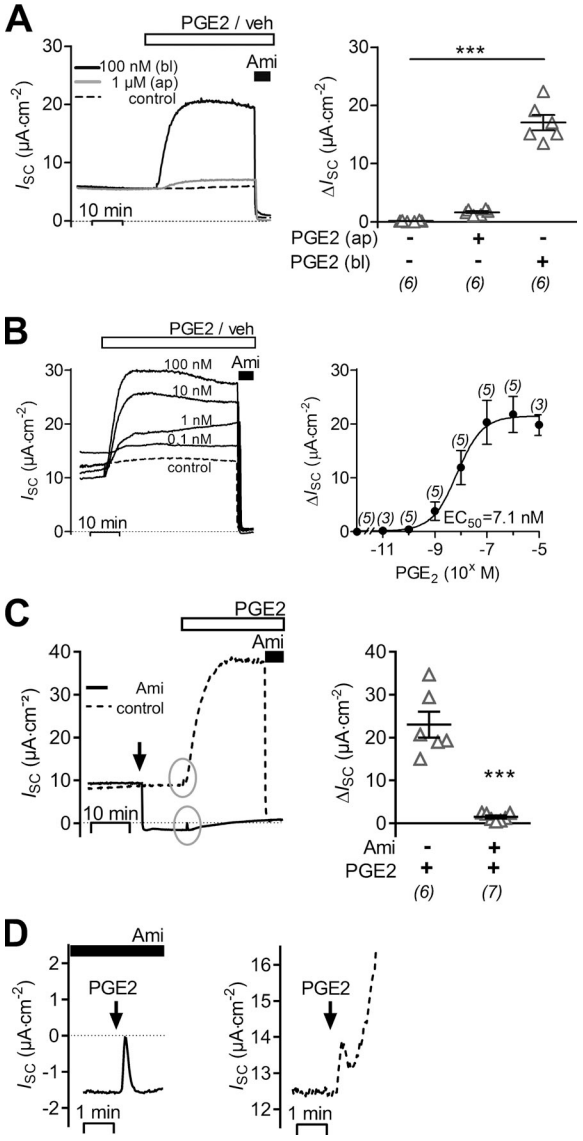

Figure 1. **Basolateral PGE_2 stimulates amiloride-sensitive I_{SC} in $mCCD_{cl1}$ cells. (A–C)** Representative traces of continuous I_{SC} recordings from $mCCD_{cl1}$ cells are shown in the left panels and data from similar experiments are summarized in the corresponding right panels. During the time periods indicated by the open horizontal bar, PGE_2 or vehicle (veh) was present. Apical application of 10 µM amiloride (Ami) is indicated by a black horizontal bar. (**A**) I_{SC} recordings with basolateral PGE_2 (bl; 100 nM), apical PGE_2 (ap; 1 µM) or vehicle (control) are represented by a black, gray, or dashed line, respectively. **(B)** I_{SC} recordings are shown with basolateral application of PGE_2 (black lines) in concentrations from 0.1–100 nM or with vehicle (dashed line). A nonlinear fit for the I_{SC} response upon PGE_2 application in concentrations of 10 pM to 10 µM was used to estimate EC_{50}. **(C)** Basolateral PGE_2 (100 nM) was applied in the absence (control; dashed line) or presence of 10 µM amiloride (black line). Arrow indicates time point of apical addition of amiloride or vehicle (control). In the control PGE_2 recording, apical amiloride (10 µM) was added at the end of the experiment. To summarize data from different experiments as ΔI_{SC} values, the individual I_{SC} values were corrected by subtracting the corresponding baseline I_{SC} value. Gray circles highlight the initial phases of the I_{SC} responses to PGE_2. Summary data (right panels) are presented as individual data points and/or mean values ± SEM. Numbers of experiments are given in parenthesis. Statistical analysis was determined using one-way ANOVA with Tukey's multiple comparison test or Student's *t* test where appropriate; ***, $P < 0.001$. **(D)** The initial phases of the responses to basolateral PGE_2 encircled in C are shown enlarged using expanded scales. Arrows indicate the time point of PGE_2 application in the continuous presence (black bar, left panel) or absence (right panel) of amiloride.

All samples were measured as duplicates.

Data analysis

Data were analyzed using PRISM 5.04 for Windows (GraphPad Software). Summarized data are presented as mean values ± SE (SEM). Multiple comparisons were subjected to one-way ANOVA followed by ad hoc post-tests as specified in the figure legends; otherwise, Student's *t* tests were used. P values < 0.05 were required to reject the null hypothesis; *, **, and *** represent P values < 0.05, 0.01, and 0.001, respectively, and "ns" represents P values ≥ 0.05. Numbers in parentheses in the figures signify the number of samples studied.

Results

Basolateral application of PGE_2 stimulates ENaC-mediated transepithelial sodium transport in $mCCD_{cl1}$ cells

Basolateral application of 100 nM PGE_2 caused a sustained increase of I_{SC} (Fig. 1 A), which rose from a baseline value of 6.7 ± 0.7 µA·cm^{-2} to a maximal value of 23.7 ± 2.1 µA·cm^{-2} ($n = 6$, $P < 0.001$) within 5–10 min. This I_{SC} increase of 17.0 ± 1.3 µA·cm^{-2} was associated with a decrease in R_{te} from 6.49 ± 0.41 to 2.61 ± 0.18 kΩ·cm^2 ($P < 0.001$). In contrast, in matched vehicle-treated control cells I_{SC} and R_{te} remained stable (6.3 ± 0.9 µA·cm^{-2} and 6.40 ± 0.54 kΩ·cm^2 versus 6.4 ± 0.9 µA·cm^{-2} and 6.34 ± 0.54 kΩ·cm^2; $n = 6$). Importantly, apical application of PGE_2 in a concentration of up to 1 µM had negligible effects on I_{SC} (Fig. 1 A). This indicates that the stimulatory effect of PGE_2 is mediated by a basolateral receptor. Apical application of amiloride (10 µM) at the end of the experiments almost completely inhibited baseline I_{SC} in vehicle-treated cells and the stimulated I_{SC} in PGE_2-treated cells. The inhibitory effect of amiloride on I_{SC} was accompanied by a 1.7-fold R_{te} increase in vehicle-treated cells (from 6.34 ± 0.54 kΩ·cm^2 to 10.56 ± 0.45 kΩ·cm^2, $n = 6$; $P < 0.001$) and a 2.6-fold R_{te} increase in PGE_2-treated cells (from 2.61 ± 0.18 kΩ·cm^2 to 6.69 ± 0.18 kΩ·cm^2, $n = 6$; $P < 0.001$). Thus, the stimulatory effect of basolateral PGE_2 on I_{SC} can be attributed to an increase in ENaC-mediated transepithelial sodium transport most likely due to an activation of ENaC activity. The latter conclusion is supported by the associated decrease in R_{te} most likely reflecting an increased sodium conductance of the apical cell membrane. As illustrated in Fig. 1 B, the stimulatory effect of basolateral PGE_2 was concentration dependent, with a half-maximal effective concentration (EC_{50}) of ∼7.1 nM. Furthermore, the PGE_2-induced increase in I_{SC} was prevented when apical application of amiloride preceded addition of PGE_2 (Fig. 1 C), which confirms that the stimulatory effect of PGE_2 is dependent on ENaC function. Interestingly, a small and transient I_{SC} peak response to PGE_2 was consistently observed in the presence of amiloride (Fig. 1 C, left panel; and Fig. 1 D, left panel). It was not an experimental artifact, because it was not observed in vehicle-treated controls. This amiloride-insensitive I_{SC} component is most likely due to a transient chloride secretory response mediated by Ca^{2+}-

activated chloride channels (Sandrasagra et al., 2004; Mansley et al., 2015). A close inspection of the initial phase of the I_{SC} response to PGE_2 revealed that a similar initial I_{SC} peak was also detectable in the absence of amiloride (Fig. 1 D, right panel). However, this I_{SC} peak response was highly variable and in most recordings was at least partially concealed by the overlapping rapid onset of the much larger stimulatory effect of PGE_2 on the amiloride-sensitive ENaC-mediated I_{SC}. Therefore, it was not feasible to study this peak response systematically. Taken together, these data indicate that in $mCCD_{cl1}$ cells basolateral PGE_2 predominantly stimulates ENaC-mediated transepithelial sodium transport most likely by increasing apical ENaC activity.

PGE_2 increases the abundance of β-ENaC at the plasma membrane

An increase in the activity of ENaC can be caused by increasing the open probability of the channel (P_O), by increasing the number of channels at the cell surface (N), or by a combination of both factors. Using a biotinylation assay and Western blot analysis with antibodies directed against mouse β-ENaC, an increase (~2.5 times) of β-ENaC protein was detected at the apical surface of cells treated with 100 nM PGE_2 on the basolateral side compared with vehicle-treated cells (Fig. 2, A and B). In the corresponding cytosolic fractions, a difference in the abundance of β-ENaC was not detected (data not shown). These data indicate that the stimulatory effect of PGE_2 on ENaC can be attributed at least in part to an increased channel expression at the apical plasma membrane of $mCCD_{cl1}$ cells.

PGE_2 mediates its effects via basolateral EP_4 receptors

To identify the prostanoid receptor responsible for the stimulatory effect of PGE_2 on ENaC activity in $mCCD_{cl1}$ cells, a pharmacological approach with known receptor agonists and antagonists was used. Basolateral addition of an EP_2 receptor antagonist (AH6809; 10 µM), which also shows some affinity to murine EP_1 receptor (Kiriyama et al., 1997), or of sulprostone (100 nM), an agonist of EP_1 and EP_3 receptors, had no effect on baseline I_{SC} and did not alter the stimulatory response to PGE_2 (Fig. 3). In contrast, the EP_4 receptor antagonists AH23848 (100 µM) or GW627368X (2 µM) largely diminished or nearly abolished the PGE_2-mediated stimulatory response, respectively (Fig. 4 A). The small transient peak response to PGE_2 appeared to be preserved in the presence of the EP_4 receptor antagonist GW627368X (Fig. 4 A, middle panel). Basolateral application of TCS2510 (100 nM), an EP_4 receptor agonist, stimulated the amiloride-sensitive current in a similar manner as PGE_2 (Fig. 4 B). These data indicate that PGE_2 stimulates ENaC activity via a basolateral $G_{\alpha s}$-coupled EP_4 receptor in $mCCD_{cl1}$ cells.

The stimulatory effect of PGE_2 on ENaC is similar to that of vasopressin and forskolin and is associated with an increase in intracellular cAMP

It has previously been reported that in $mCCD_{cl1}$ cells, ENaC-mediated transepithelial sodium transport can be stimulated by vasopressin via a basolateral V2 receptor (Gaeggeler et al., 2011). Therefore, experiments were performed to compare the

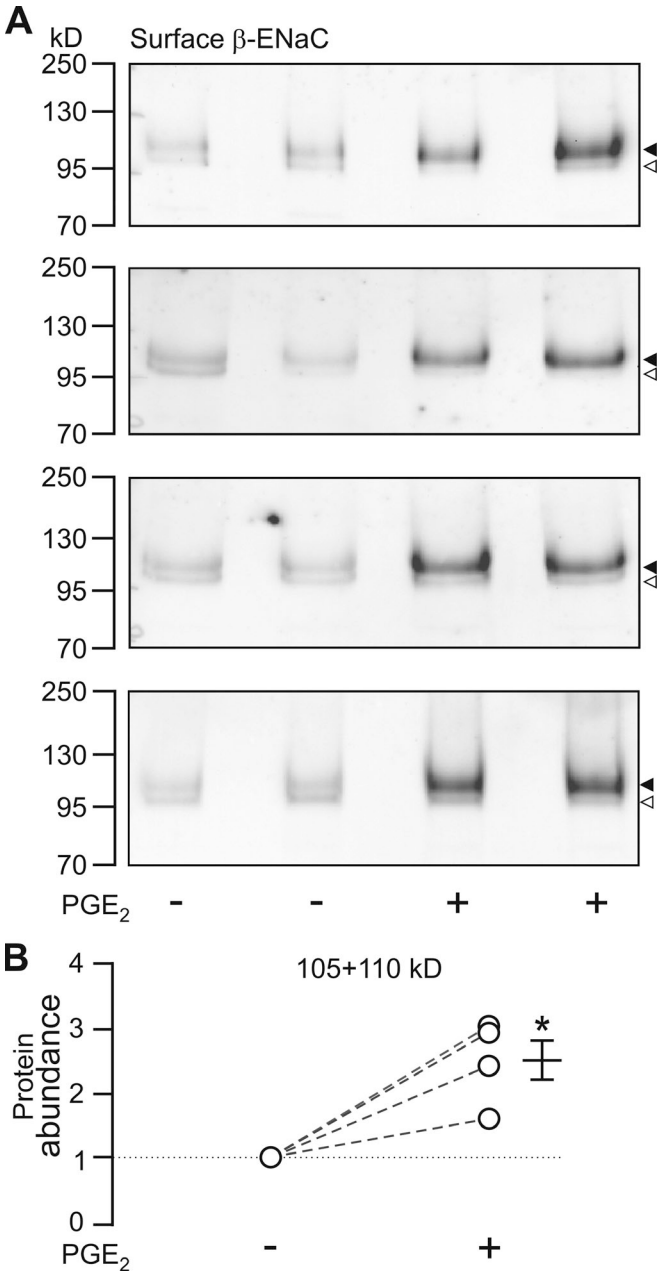

Figure 2. **PGE_2 elevates the abundance of β-ENaC at the cell surface. (A)** β-ENaC was detected by Western blot analysis using biotinylated cell surface proteins isolated from $mCCD_{cl1}$ cells exposed on the basolateral side for 30 min to 100 nM PGE_2 (+) or vehicle (–). The four blots represent data from four individual experiments using two filters of $mCCD_{cl1}$ cells per experimental group. Arrowheads to the right of the blots indicate band sizes of ~110 kD (filled) and ~105 kD (open) as expected for glycosylated and nonglycosylated β-ENaC. **(B)** The blots shown in A were analyzed by densitometry, and the signals of the lower and upper bands of each lane were combined (105 + 110 kD). In each experiment, two matched $mCCD_{cl1}$ samples were used per group (± PGE_2) and an average value was determined for each group. For each experiment, the average value from the PGE_2-treated cells was normalized to the average value of the nontreated cells (corresponding values are connected by a dashed line). The mean ± SEM value represents the average change in protein abundance compared with vehicle treatment. Statistical analysis was performed using Student's *t* test; *, $P < 0.05$ versus solvent vehicle controls.

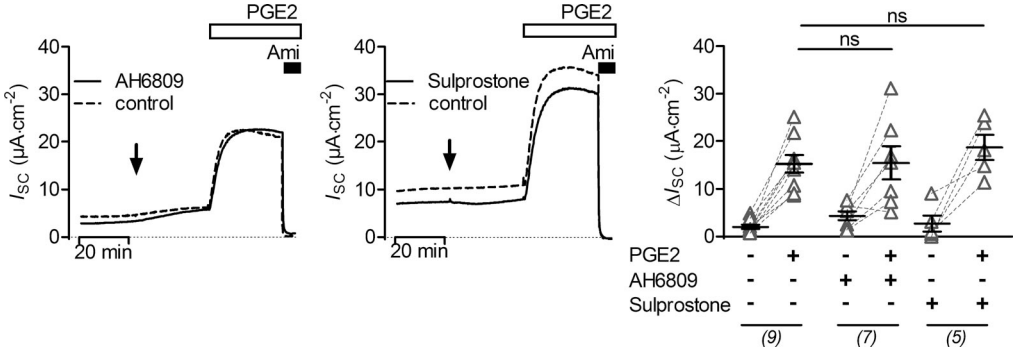

Figure 3. **EP_1, EP_2, and EP_3 receptors are not involved in mediating the stimulatory effect of PGE_2 on ENaC.** In the left and middle panels, representative I_{SC} recordings are shown. At the time point indicated by an arrow, cells were exposed to 10 µM AH6809 (EP_2 receptor antagonist; left panel, solid line), 100 nM sulprostone (EP_1/EP_3 receptor agonist; middle panel, solid line), or vehicle in matched control recordings (control, dashed line). Approximately 30 min later, all cells were exposed to 100 nM basolateral PGE_2 and subsequently to apical amiloride (Ami; 10 µM) as indicated. Summary data (right panel) are presented as ΔI_{SC} values, which were determined by subtracting the corresponding baseline I_{SC} from the I_{SC} reached in the presence (+) or absence (–) of PGE_2, AH6809, and sulprostone as indicated. Data are presented as individual values and their mean ± SEM; paired data are connected by dashed lines. Numbers of experiments are given in parenthesis. ns, P > 0.05, one-way ANOVA with Tukey's multiple comparison test.

effect of vasopressin with that of PGE_2 and to investigate a possible interdependence of these effects. First, the stimulatory effect of vasopressin was confirmed (Fig. 5, A and B). Basolateral application of 25 pM vasopressin increased I_{SC} to a similar extent as 100 nM basolateral PGE_2 in matched experiments. Interestingly, exposure to PGE_2 after prestimulation with vasopressin had no additional stimulatory effect on I_{SC} (Fig. 5 A). Similarly, when cells were initially exposed to PGE_2, subsequent application of vasopressin failed to stimulate I_{SC} further (Fig. 5 B). These findings suggest that the effects of PGE2 and vasopressin involve the same signaling pathway, i.e., cAMP/PKA. To confirm this, further experiments were performed with forskolin, a known activator of AC. Forskolin (10 µM) increased I_{SC} in a similar manner as vasopressin and PGE_2 (Fig. 5 C). After exposure to forskolin, application of PGE_2 (100 nM) had no additional stimulatory effect. To provide evidence that PGE_2 causes an increase in intracellular cAMP, an enzyme immunoassay was used. Indeed, in PGE_2-treated $mCCD_{cl1}$ cells cytosolic cAMP concentration was elevated to 137.6 ± 47.2 fmol/µg whole-cell protein compared with 9.5 ± 3.8 fmol/µg whole-cell protein in matched vehicle-treated control cells (n = 3).

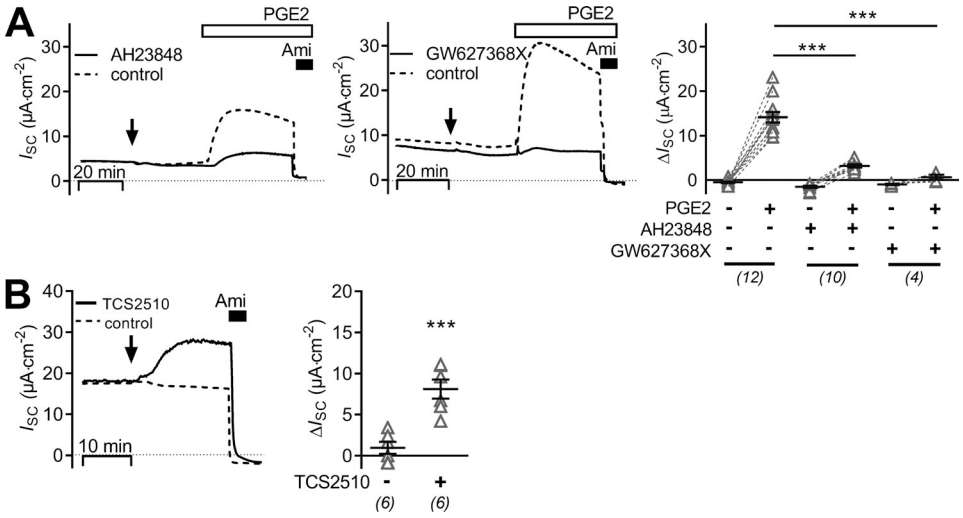

Figure 4. **PGE_2 stimulates ENaC activity via basolateral EP_4 receptors. (A)** The left and middle panel show representative I_{SC} recordings in which vehicle (control; dashed lines) or EP_4 receptor antagonists (100 µM AH23848 or 2 µM GW627368X; solid lines) were added basolaterally at the time point indicated by an arrow. Approximately 30 min later, all cells were exposed to 100 nM basolateral PGE_2 and subsequently to apical amiloride (Ami; 10 µM) as indicated. Summary data (right panel) are presented as ΔI_{SC} values, which were determined by subtracting the corresponding baseline I_{SC} from the I_{SC} reached in the presence (+) or absence (–) of PGE_2, AH23848, and GW627368X as indicated. **(B)** Representative I_{SC} recordings (left panel) from cells exposed basolaterally to the EP_4 receptor agonist TCS2510 (solid line; 100 nM) or vehicle (control, dashed line) at the time point indicated by the arrow. Apical amiloride (10 µM) was applied as indicated. Summary data (right panel) are presented as ΔI_{SC} values determined by subtracting the corresponding baseline I_{SC} from the I_{SC} reached after treating cells with TCS2510 (+) or vehicle (–). Data are presented as individual values and their mean ± SEM; paired data are connected by dashed lines. Numbers of experiments are given in parentheses. ***, P < 0.001, one-way ANOVA with Tukey's multiple comparison test.

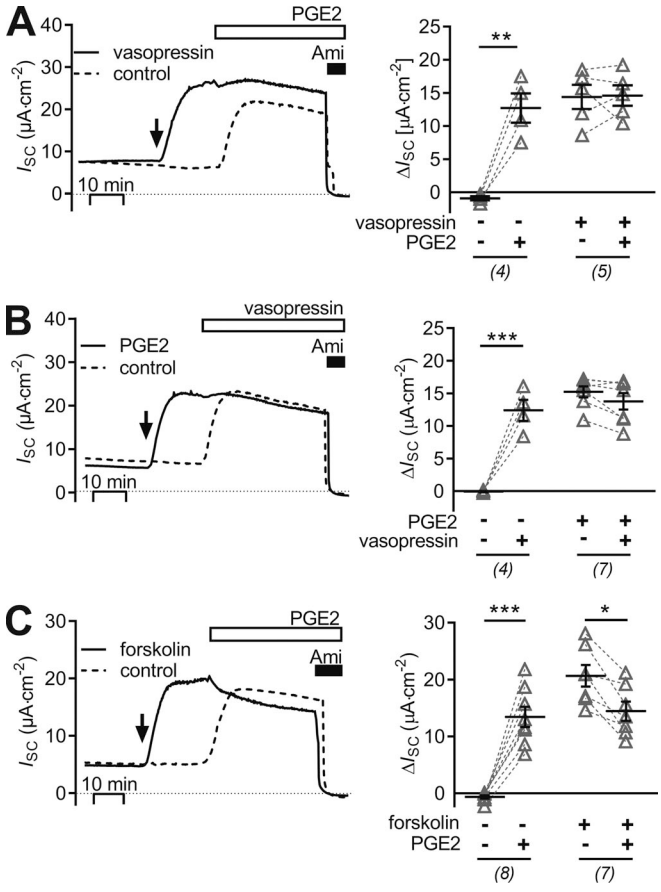

Figure 5. **The stimulatory effect of PGE_2 is similar and not additive to those of vasopressin and forskolin. (A–C)** Representative traces of continuous I_{SC} recordings from $mCCD_{cl1}$ cells are shown in the left panels, and data from similar experiments are summarized in the corresponding right panels. **(A)** At the time point indicated by an arrow, cells were exposed to 25 pM basolateral vasopressin (solid line) or vehicle in matched control recordings (control, dashed line). About 20 min later all cells were exposed to 100 nM basolateral PGE_2 and subsequently to apical amiloride (Ami; 10 µM) as indicated. **(B)** At the time point indicated by an arrow, cells were exposed to 100 nM basolateral PGE_2 (solid line) or vehicle in matched control recordings (control, dashed line). Approximately 20 min later, all cells were exposed to 25 pM basolateral vasopressin and subsequently to apical amiloride (10 µM) as indicated. **(C)** At the time point indicated by an arrow, cells were exposed to 10 µM forskolin (solid line) to stimulate adenylyl cyclase or to vehicle in matched control recordings (control, dashed line). Approximately 20 min later, all cells were exposed to 100 nM basolateral PGE_2 and subsequently to apical amiloride (10 µM) as indicated. Summary data (right panel) are presented as ΔI_{SC} values, which were determined by subtracting the corresponding baseline I_{SC} from the I_{SC} reached in the presence (+) or absence (–) of PGE_2, vasopressin, and forskolin as indicated. Data are presented as individual values and their mean ± SEM. Paired data are connected by dashed lines. Numbers of experiments are given in parentheses. *, P < 0.05; **, P < 0.01; ***, P < 0.001, paired Student's *t* test.

The stimulatory effect of PGE_2 on ENaC activity is preserved in cells pretreated with aldosterone

As shown previously (Gaeggeler et al., 2005; Mansley et al., 2018), $mCCD_{cl1}$ cells treated with a physiological concentration of aldosterone (3 nM) responded with a sustained increase of I_{SC} from 8.7 ± 0.9 µA·cm^{-2} to 17.9 ± 1.6 µA·cm^{-2} (n = 9, P < 0.001; Fig. 6) reaching a new plateau within ∼2 h. Basolateral application of PGE_2 (100 nM) at the plateau of the aldosterone response caused a further rapid (within 5–10 min) increase in I_{SC} by 16.8 ± 1.1 µA·cm^{-2}. This stimulatory effect of PGE_2 in aldosterone-treated cells was similar to that in matched vehicle-treated control cells, averaging 17.3 ± 1.5 µA·cm^{-2} (n = 11; Fig. 6). These results indicate that the stimulatory effect of PGE_2 on ENaC is independent of the signaling pathways mediating the stimulatory effect of aldosterone.

PGE_2 is generated and secreted by $mCCD_{cl1}$ cells exposed to the precursor arachidonic acid and stimulates ENaC activity in an autocrine manner

The finding that exogenously applied PGE_2 stimulates ENaC activity in $mCCD_{cl1}$ cells raised the question whether endogenously generated prostanoids may elicit a similar response. To promote the synthesis of endogenous PGE_2, its precursor arachidonic acid was applied at a concentration of 50 µM. At this concentration, arachidonic acid is not rate limiting for the biosynthesis of PGE_2 (Bonvalet et al., 1987). Apical application of arachidonic acid increased I_{SC} from 9.8 ± 1.5 µA·cm^{-2} to 25.1 ± 2.4 µA·cm^{-2} (n = 8, P > 0.001; Fig. 7 A, dashed line). The stimulated I_{SC} was inhibited by amiloride, which indicates that the stimulatory effect of arachidonic acid is due to increased ENaC-mediated transepithelial sodium transport. The stimulatory effect of arachidonic acid was similar to that of PGE_2, and subsequent application of PGE_2 (100 nM) to the basolateral bath did not increase I_{SC} further (ΔI_{SC} = –1.5 ± 0.6 µA·cm^{-2}). Importantly, treating $mCCD_{cl1}$ cells with the COX-1/2 inhibitor indomethacin (50 µM) completely prevented the stimulatory response to arachidonic acid (ΔI_{SC} = 0.3 ± 0.2 µA·cm^{-2}, n = 8; Fig. 7 A, solid line). In contrast, the stimulatory effect of subsequently applied PGE_2 was fully preserved (ΔI_{SC} =10.7 ± 1.3 µA·cm^{-2}, n = 8). Thus, $mCCD_{cl1}$ cells are capable of synthesizing and releasing a COX-derived prostanoid, most likely PGE_2, which can stimulate ENaC activity in an autocrine manner, preventing a further stimulation by exogenous PGE_2. This hypothesis is further supported by the finding that the stimulatory effect of arachidonic acid was largely reduced in the presence of the EP_4 receptor antagonists AH23848 (100 µM) and GW627368X (2 µM) in the basolateral solution (Fig. 7 B). In $mCCD_{cl1}$ cells, we did not observe an inhibitory effect of arachidonic acid on ENaC-mediated I_{SC}. In contrast, ENaC inhibition via cytochrome P450 epoxygenase-dependent pathways has been reported in microdissected rat CCD (Wei et al., 2004) and mpkCCD cells (Pavlov et al., 2011). The lack of an inhibitory effect in $mCCD_{cl1}$ cells cannot be attributed to an insufficient concentration of arachidonic acid used in our experiments because in rat CCD, the concentration required to inhibit ENaC activity by 50% was ∼2 µM.

In additional experiments cell culture medium was collected from the basolateral bath of cells treated with apical arachidonic acid (donor cells). The collected medium was transferred to the basolateral compartment of nontreated $mCCD_{cl1}$ cells (receiver cells) in a 1:1 (vol/vol) ratio. This resulted in a significant stimulation of I_{SC} in the receiver cells (ΔI_{SC} = 5.6 ± 1.4 µA·cm^{-2}, n = 7). Subsequent application of PGE_2 had an additional but less pronounced stimulatory effect on I_{SC}. The stimulatory effect of medium from donor cells was preserved when COX-1/2 activity

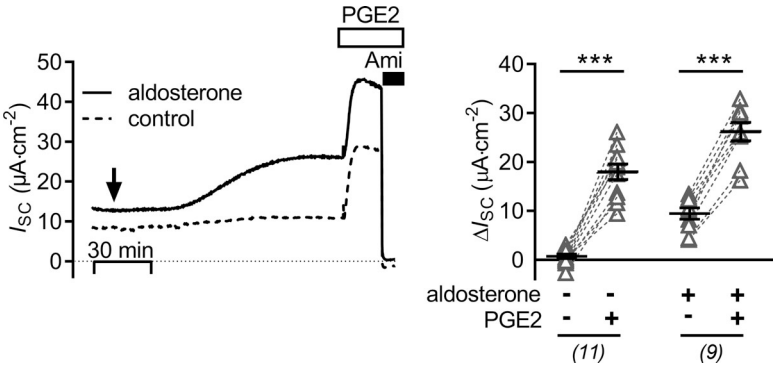

Figure 6. **The stimulatory effect of PGE_2 upon ENaC activity is preserved in cells pretreated with aldosterone.** The left panel shows representative I_{SC} recordings in which vehicle (control; dashed line) or aldosterone (3 nM; solid line) were added bilaterally at the time point indicated by an arrow. Approximately 2 h later, cells were exposed to 100 nM basolateral PGE_2 and subsequently to apical amiloride (Ami; 10 μM) as indicated. Summary data (right panel) are presented as ΔI_{SC} values, which were determined by subtracting the corresponding baseline I_{SC} from the I_{SC} reached in the presence (+) or absence (–) of aldosterone and PGE_2 as indicated. Data are presented as individual values and their mean ± SEM. Paired data are connected by dashed lines. Numbers of experiments are given in parentheses. ***, P < 0.001, paired Student's *t* test.

in the receiver cells was inhibited by indomethacin (ΔI_{SC} 5.4 ± 1.3 μA·cm^{-2}, *n* = 7; Fig. 7 C). This rules out the possibility that the stimulatory effect of the transferred medium was mediated by a contamination with arachidonic acid. Finally, the stimulatory effect of the transferred medium on ENaC activity was largely abolished when the receiver cells were pretreated with the EP_4 receptor antagonist GW627368X in the basolateral bath (ΔI_{SC} = of 1.4 ± 0.5 μA·cm^{-2}). In contrast, medium transfer increased I_{SC} by 12.4 ± 1.3 μA·cm^{-2} in nontreated matched control cells (*n* = 4, P < 0.001; Fig. 7 D).

Stimulation of ENaC in $mCCD_{cl1}$ cells by arachidonic acid requires COX-1 activity

Similar to treating $mCCD_{cl1}$ cells with the nonselective COX-1/2 inhibitor indomethacin (Fig. 7 A), treating cells with the selective COX-1 inhibitor SC-560 (0.14 μM; Fig. 8 A) largely prevented the stimulatory effect of arachidonic acid on ENaC activity. The arachidonic acid–induced ΔI_{SC} was reduced to 4.4 ± 0.6 μA·cm^2 (*n* = 6) compared with the effect of arachidonic acid in matched controls with a ΔI_{SC} of 17.1 ± 2.7 μA·cm^2 (*n* = 7, P < 0.05). In contrast, lumiracoxib (2 μM; Fig. 8 B), a highly selective COX-2 inhibitor, did not prevent the stimulatory effect of arachidonic acid. Indeed, in cells treated with lumiracoxib, the effect of arachidonic acid was preserved with a ΔI_{SC} of 15.7 ± 2.7 μA·cm^{-2} (*n* = 6), which was not different from the ΔI_{SC} of 18.9 ± 2.7 μA·cm^{-2} (*n* = 6) elicited by arachidonic acid in vehicle-treated control cells. These data indicate that COX-1 is the dominant isoenzyme involved in PGE_2 generation in $mCCD_{cl1}$ cells. To confirm synthesis and basolateral secretion of PGE_2, its concentration was measured in the basolateral culture medium of $mCCD_{cl1}$ cells. The concentration of PGE_2 in the basolateral medium of $mCCD_{cl1}$ cells exposed to apical arachidonic acid was significantly higher (16.3 ± 3.8 nmol·l^{-1}, *n* = 6) than that of vehicle-treated control cells (0.3 ± 0.2 nmol·l^{-1}, *n* = 8, P < 0.01; Fig. 8 C). The arachidonic acid–dependent increase in basolateral PGE_2 concentration was abolished by the COX-1 inhibitor SC-560 (0.3 ± 0.1 nmol·l^{-1}, *n* = 7, P < 0.001), but not by the COX-2 inhibitor lumiracoxib (7.4 ± 5.4 nmol·l^{-1}, *n* = 7, P > 0.05), which is consistent with the I_{SC} data reported above.

Transcripts for EP receptors and for enzymes of the PGE_2 biosynthetic pathway were detected in $mCCD_{cl1}$ cells

RT-PCR experiments revealed the presence of transcripts for EP_4 and EP_1 receptors in $mCCD_{cl1}$ cells. In contrast, transcripts for EP_2 or EP_3 receptors were not detected (Fig. 9 A). Moreover, transcripts for several enzymes (COX-1, COX-2, mPGES2, and cPGES) involved in the biochemical pathway of PGE_2 synthesis were detected not including mPGES1 (Fig. 9 B). Targets were confirmed by extracting and sequencing the PCR bands of interest.

Discussion

The present study provides evidence that basolateral, but not apical application of PGE_2 stimulates ENaC-dependent transepithelial sodium transport in $mCCD_{cl1}$ cells. Moreover, it demonstrates that this stimulatory effect is mediated by EP_4 receptor signaling and is due to increased ENaC activity resulting, at least in part, from enhanced channel expression at the apical cell surface. Finally, experiments with the PGE_2 precursor arachidonic acid indicate that $mCCD_{cl1}$ cells can synthesize and release PGE_2 to stimulate transepithelial sodium transport in an autocrine manner.

The sustained stimulatory effect of PGE_2 on ENaC-mediated I_{SC} in $mCCD_{cl1}$ cells is reminiscent of similar effects previously observed in *Xenopus laevis* A6 (Kokko et al., 1997; Matsumoto et al., 1997) and canine MDCK renal epithelial cells (Wegmann and Nüsing, 2003). This challenges the view that PGE_2 mainly inhibits sodium absorption in the collecting duct. Interestingly, an inhibitory effect of PGE_2 on sodium absorption was not observed in isolated perfused rat CCD (Chen et al., 1991). Moreover, the inhibitory effects of PGE_2 on Na^+ transport in microdissected rabbit tubules (Stokes and Kokko, 1977; Iino and Imai, 1978) and primary cultures of rabbit principal CCD cells (Ling et al., 1992) were short-term, occurring within a few minutes of basolateral PGE_2 application. In contrast, the stimulatory effect observed in $mCCD_{cl1}$ cells in the present study reached a maximum within ~10 min and was sustained. In this context, it is of interest that a biphasic action of PGE_2 has been reported in *Xenopus* A6 renal epithelial cells with an acute inhibition (3–6 min) and a delayed stimulation (10–50 min) of ENaC by basolateral PGE_2 (Kokko et al., 1994, 1997; Worrell et al., 2001). The acute inhibition is probably caused by an increase in intracellular Ca^{2+} signaling. In contrast, the delayed stimulatory effect is due to an increase in intracellular cAMP leading to an increase in the number of channels expressed in the apical membrane (Kokko et al., 1994).

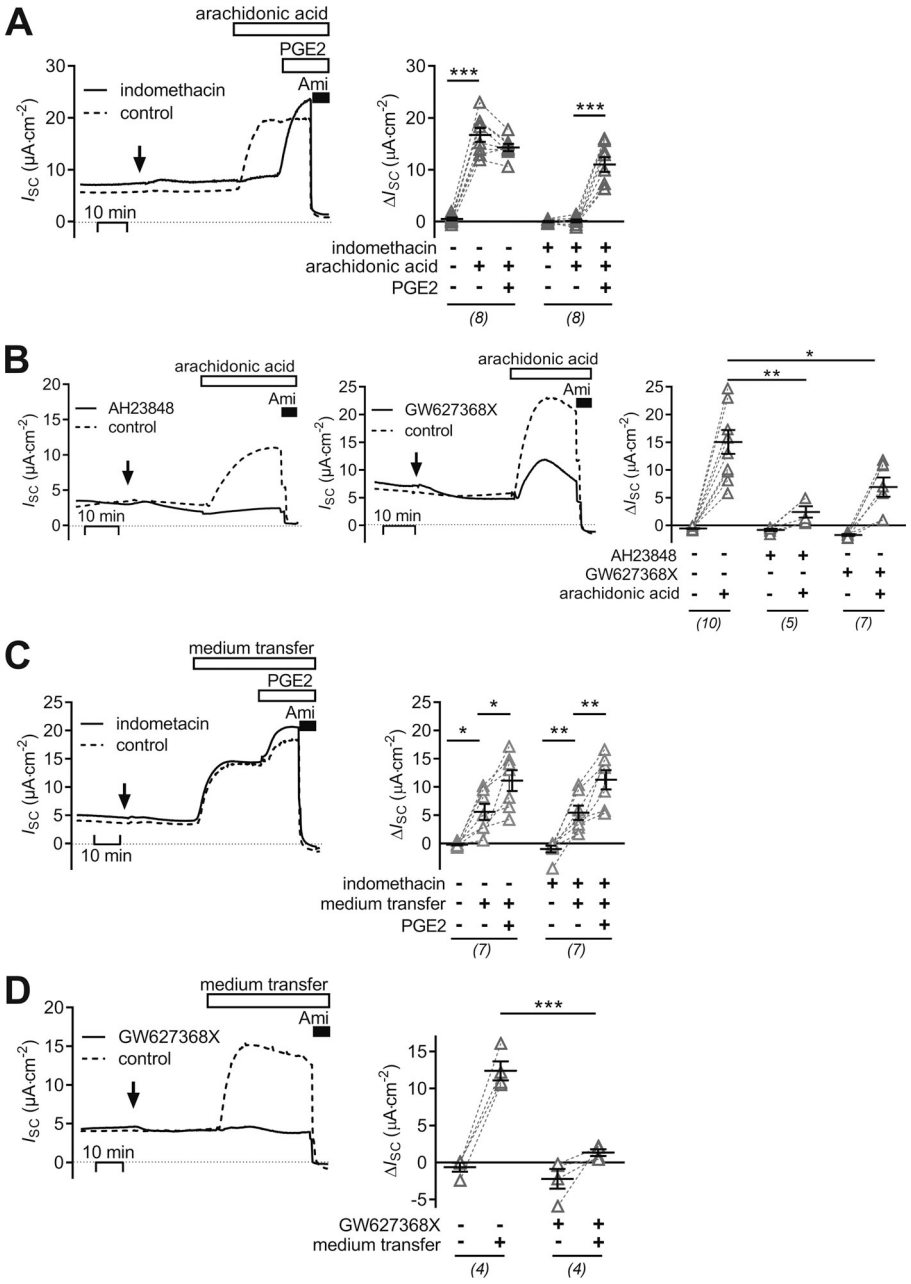

Figure 7. **Stimulation of ENaC activity in $mCCD_{cl1}$ cells by arachidonic acid is mediated via basolateral EP_4 receptors and constitutively active COX.** The left panel in A and the left and middle panels in B show representative traces of continuous I_{SC} recordings. 50 µM indomethacin (A) or 100 µM AH23848 or 2 µM GW627368X (B; solid lines) was added basolaterally at the time point indicated by an arrow. Dashed lines indicate matched control recordings treated with the respective vehicle (control). About 30 min later cells were exposed to 50 µM apical arachidonic acid and in A followed by basolateral 100 nM PGE_2. Finally, apical 10 µM amiloride was added as indicated. Summary data (right panel) are presented as ΔI_{SC} values, which were determined by subtracting the corresponding baseline I_{SC} from the I_{SC} reached in the presence (+) or absence (–) of indomethacin, arachidonic acid, PGE_2, AH23848, and GW627368X as indicated. The left panels in C and D show representative traces of continuous I_{SC} recordings in which vehicle (control; dashed lines), 50 µM indomethacin, or 2 µM GW627368X (solid lines) was added basolaterally at the time point indicated by an arrow. Approximately 30 min later, medium from the basolateral compartment of a second set of cells (donor cells; not depicted) which were treated with apical 50 µM arachidonic acid was transferred to the basolateral compartment (indicated as medium transfer) in a 1:1 (vol/vol) ratio. This was followed in C by basolateral 100 nM PGE_2. Finally, as indicated, 10 µM amiloride was applied to all cells. Summary data (right panel) are presented as ΔI_{SC} values, which were determined by subtracting the corresponding baseline I_{SC} from the I_{SC} reached in the presence (+) or absence (–) of indomethacin, GW627368X, PGE_2, and medium transfer as indicated. Summary data are presented as individual values and their mean ± SEM. Paired data are connected by dashed lines. Numbers of experiments are given in parentheses. ***, $P < 0.001$; **, $P < 0.01$; *, $P < 0.05$, one-way ANOVA with Tukey's multiple comparison test or unpaired Student's *t* test, where appropriate.

This latter interpretation is in good agreement with our observation in $mCCD_{cl1}$ cells.

In a previous study, our group reported that PGE_2 stimulates Cl^- secretion in murine M-1 CCD cells (Sandrasagra et al., 2004). In this latter study, no stimulatory effect of PGE_2 on the amiloride-sensitive I_{SC} component was observed. A possible explanation for this discrepancy is that in M-1 cells, ENaC-dependent I_{SC} is usually maximally stimulated under baseline conditions, which makes it difficult to detect any additional stimulatory effects on ENaC. A prestimulation of ENaC by deoxycorticosterone acetate in the majority of experiments may be a reason why no stimulatory effect of 10–100 nM PGE_2 was detected in isolated rabbit collecting tubules (Stokes and Kokko, 1977; Iino and Imai, 1978). Moreover, in our previous study (Sandrasagra et al., 2004), we focused on the short-term effects of PGE_2 and may have overlooked a delayed stimulatory response. In $mCCD_{cl1}$ cells the sustained I_{SC} increase in response to PGE_2 is clearly due to a stimulatory effect on ENaC. This is evidenced by the finding that the response could not be elicited in the presence of amiloride and that the PGE_2-stimulated I_{SC} was completely inhibited by amiloride. In contrast, a minor rapid and transient I_{SC} peak preceding the sustained stimulatory response to PGE_2 was preserved in the presence of amiloride or in the presence of the EP4 receptor antagonist GW627368X. This suggests that the transient peak response is not mediated by EP_4 and reflects electrogenic Cl^- secretion reminiscent of the Cl^- secretory response observed in M-1 cells (Sandrasagra et al., 2004). Thus, under certain conditions, $mCCD_{cl1}$ cells, like M-1 cells and mouse inner medullary collecting duct cells (Rajagopal et al., 2014), may have the ability to secrete Cl^- in response to

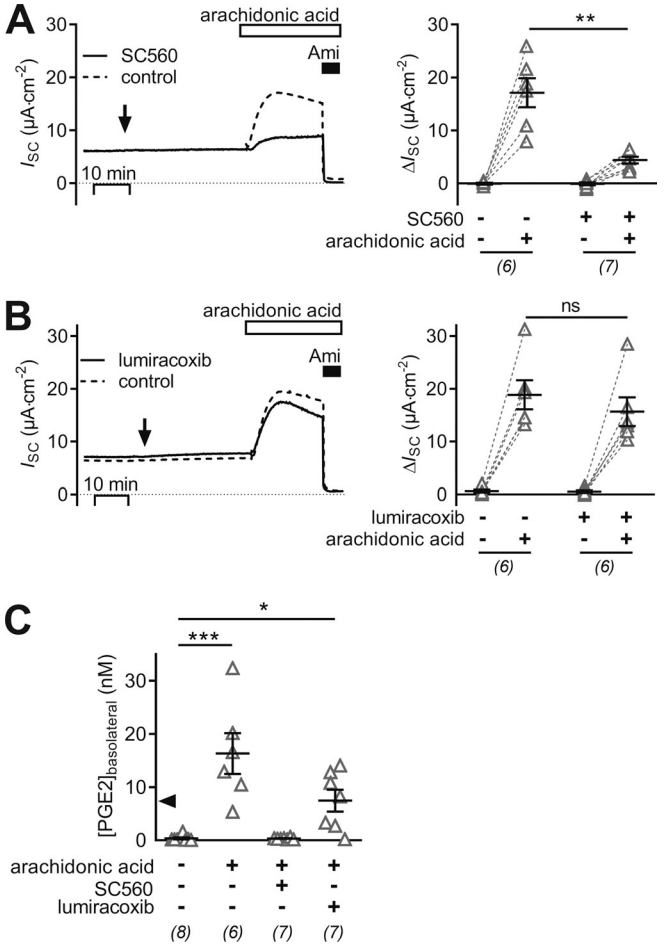

Figure 8. **Stimulation of ENaC in mCCD$_{cl1}$ cells by arachidonic acid requires COX-1 activity. (A and B)** Representative traces of continuous I_{SC} recordings from mCCD$_{cl1}$ cells are shown in the left panels, and data from similar experiments are summarized in the corresponding right panels. At the time point indicated by an arrow, cells were exposed to 0.14 µM SC560 (COX-1 selective inhibitor, solid line) or vehicle in matched control recordings (A; control, dashed line) or 2 µM lumiracoxib (COX-2 selective inhibitor, solid line) or vehicle in matched control recordings (B; control, dashed line). Approximately 30 min later, all cells were exposed to 50 µM apical arachidonic acid and subsequently to apical amiloride (Ami; 10 µM) as indicated. Summary data (right panel) are presented as ΔI_{SC} values, which were determined by subtracting the corresponding baseline I_{SC} from the I_{SC} reached in the presence (+) or absence (–) of SC560, lumiracoxib, and arachidonic acid as indicated. **(C)** Concentration of PGE_2 measured in basolateral cell culture medium collected from cells in the presence (+) or absence (–) of 50 µM arachidonic acid, 0.14 µM SC560 and 2 µM lumiracoxib as indicated. The solid arrowhead indicates the EC_{50} value for the I_{SC} response upon PGE_2 as determined in Fig. 1. Data are presented as individual values and their mean ± SEM. Numbers of experiments are given in parentheses. ***, P < 0.001; **, P < 0.01; *, P < 0.05; ns, P ≥ 0.05, one-way ANOVA with Dunn's multiple comparison test.

PGE_2. However, in mCCD$_{cl1}$ cells, the predominant effect of PGE_2 is a substantial and sustained stimulation of ENaC-dependent Na^+ absorption. Importantly, the estimated EC_{50} of ~7.1 nM for this stimulatory PGE_2 effect is within a range that may be relevant in vivo (Bonvalet et al., 1987).

The present study provides pharmacological evidence that the stimulatory effect of PGE_2 on ENaC is mediated by EP_4 receptors in the basolateral membrane of mCCD$_{cl1}$ cells. This conclusion is further supported by the finding that PGE_2 caused an increase in intracellular cAMP as expected for a $G_{\alpha s}$-coupled receptor. In agreement with the functional data, transcripts for EP_4 receptor were detected in mCCD$_{cl1}$ cells consistent with previous reports of EP_4 receptor expression in the collecting duct (Jensen et al., 2001; Hao and Breyer, 2008). In contrast, transcripts for EP_2 or EP_3 receptors were not detected in mCCD$_{cl1}$ cells. The absence of EP_2 receptor transcripts is plausible, because renal EP_2 receptor expression is thought to be limited to interstitial cells and the vasculature (Li et al., 2017). The lack of EP_3 receptor expression in mCCD$_{cl1}$ cells was unexpected and may not reflect the situation in the native collecting duct, where EP_3 receptor is expressed, but its cellular localization and precise physiological role is less clear (Hao and Breyer, 2008). Of interest is the detection of EP_1 receptor transcripts in mCCD$_{cl1}$ cells consistent with the reported expression of EP_1 receptor in the collecting duct (Guan et al., 1998) and M-1 cells (Sandrasagra et al., 2004). EP_1 receptor is a $G_{\alpha q/11}$-coupled receptor, and its activation leads to a rise in cytosolic Ca^{2+} via the IP_3/diacylglycerol pathway (Narumiya et al., 1999; Breyer and Breyer, 2000b). An EP1-mediated increase in intracellular calcium is thought to be the mechanism by which PGE_2 inhibits sodium absorption in rabbit and mouse CCD (Hébert et al., 1991; Guan et al., 1998; Nasrallah et al., 2018). Thus, whether PGE_2 inhibits or stimulates sodium absorption in the collecting duct may depend on the relative expression of EP1 versus EP4 receptors which may vary in different parts of the collecting duct according to physiological needs. It has been speculated that in M-1 cells the initial Cl^- secretory response to PGE_2 is mediated through EP_1 receptor activation and subsequent stimulation of Ca^{2+}-activated chloride channels (Sandrasagra et al., 2004). This may also be the mechanism underlying the small ENaC-independent transient I_{SC} response to PGE_2 occasionally observed in mCCD$_{cl1}$ cells. Presently, it is unclear whether Cl^- secretion is physiologically relevant in CCD cells or becomes relevant under pathophysiological conditions like in polycystic kidney disease, where it is thought to contribute to cyst enlargement (Liu et al., 2012; Blanco and Wallace, 2013). In contrast, it is well established that ENaC function in the CCD and its appropriate regulation play a key role in maintaining sodium homeostasis. Thus, the reported stimulatory effect of PGE_2 on ENaC-mediated transepithelial sodium transport is potentially important under certain physiological and pathophysiological conditions.

PGE_2 is the most abundant prostanoid detected in the kidney, but the physiologically relevant sites for the synthesis of PGE_2 remain to be defined (Hao and Breyer, 2008). The present study provides evidence that mCCD$_{cl1}$ cells can synthesize and secrete PGE_2. Indeed, apical exposure to the PGE_2 precursor arachidonic acid caused substantial secretion of PGE_2, which reached a concentration of ~16 nM in the basolateral culture medium of treated cells compared with ~0.3 nM in the basolateral medium of control cells. From the PGE_2 concentration reached in the basolateral medium of treated cells it can be estimated that confluent mCCD$_{cl1}$ cells, covering one tissue culture insert, secrete ~4 µg PGE_2 over a 30-min period. This corresponds to a secretion rate of ~79 fg PGE_2/ng cellular protein per 30 min. It is conceivable that this secretion rate may be achieved in vivo,

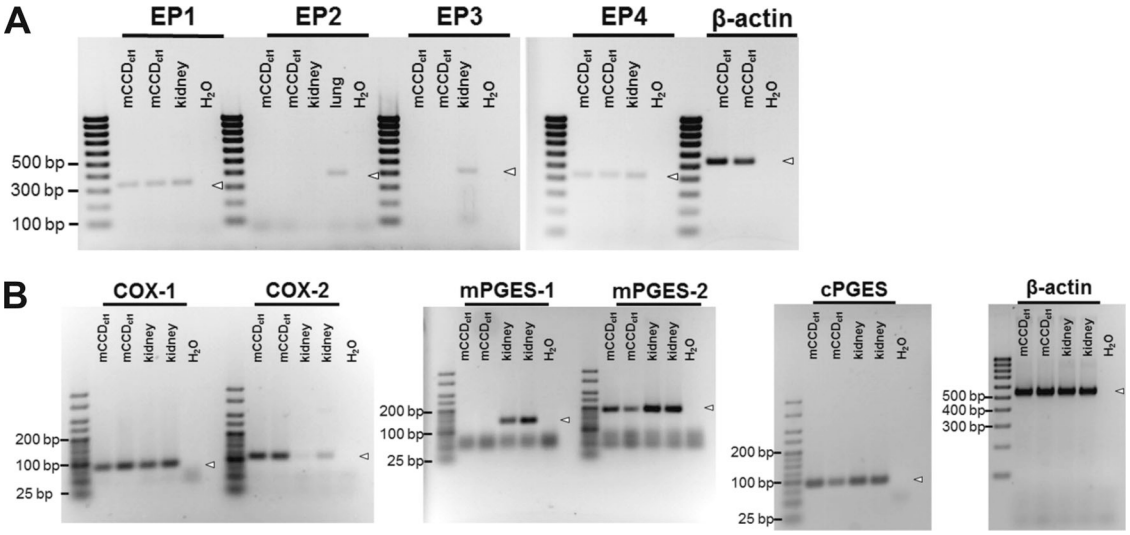

Figure 9. **Transcripts for EP receptors and for enzymes of the PGE_2 biosynthetic pathway were detected in $mCCD_{cl1}$ cells.** Specific primers were used to detect the transcript expression of the prostanoid receptors EP_1–EP_4 (A), as well as key enzymes involved in PGE_2 synthesis, namely COX-1, COX-2, mPGES1, mPGES2, and cPGES (B). Transcript expression was determined in RNA extracted from $mCCD_{cl1}$ cells, as well as from mouse cortical kidney and lung homogenates. H_2O and primers recognizing β-actin served as no-template and loading control, respectively. Expected individual transcript sizes are indicated by open arrowheads.

because synthesis rates ranging from ∼800 to >8,000 fg·ng protein^{-1}·30 min^{-1} have been reported for PGE_2 synthesis in the collecting duct (Bonvalet et al., 1987; Liu et al., 2014). In light of the EC_{50} value of ∼7.1 nM, the concentration of PGE_2 of ∼16 nM explains the robust stimulatory effect observed in medium transfer experiments when receiver cells were exposed to a 1:1 dilution of the basolateral medium from donor cells. It also explains why the stimulatory effect was submaximal and why subsequent exposure to 100 nM PGE_2 further stimulated I_{SC} in these experiments (Fig. 7 C). In contrast, in $mCCD_{cl1}$ cells exposed to arachidonic acid on the apical side subsequent exposure to 100 nM PGE_2 on the basolateral side had no additional stimulatory effect (Fig. 7 A). This is plausible, because the local PGE_2 concentration reached within the vicinity of the basolateral membrane of $mCCD_{cl1}$ cells exposed to apical arachidonic acid is probably much higher than the ∼16 nM measured in the bulk medium. Thus, autocrine secretion of PGE_2 may well be sufficient to achieve a maximal EP_4 receptor-mediated stimulatory effect on the amiloride-sensitive I_{SC} (Fig. 7).

In the renal cortex, COX-1 and downstream prostaglandin synthases are constitutively expressed, while basal expression of COX-2 is low (Yang et al., 1998; Murakami et al., 2002; Tanikawa et al., 2002; Hao and Breyer, 2008). This study provides evidence that transcripts for COX-1, mPGES2, and cPGES, but not mPGES1, are expressed in $mCCD_{cl1}$ cells. Once arachidonic acid is processed by COX-1, the biosynthesis of PGE_2 can be achieved by mPGES2 or cPGES. The stimulatory effect of arachidonic acid on ENaC-dependent I_{SC} was abolished in $mCCD_{cl1}$ cells treated with the nonselective COX-1/2 inhibitor indomethacin or the selective COX-1 inhibitor SC560. In contrast, the selective COX-2 inhibitor lumiracoxib did not prevent the stimulatory effect of arachidonic acid. These findings indicate that COX-1 plays a major role in PGE_2 synthesis in $mCCD_{cl1}$ cells, which is consistent with the finding that COX-1 is the primary isoform in native CCD (Vitzthum et al., 2002) with a preferential localization in CCD principal cells (Câmpean et al., 2003).

cPGES transcripts are ubiquitously expressed in mouse epithelial cells of the connecting tubule and collecting duct (Chen et al., 2017; Ransick et al., 2019), and immunoreactive cPGES has been detected in cultured mouse inner medullary collecting duct cells (Zhang et al., 2003). Therefore, its detection in $mCCD_{cl1}$ cells is not surprising. Interestingly, mPGES2 is thought to be primarily expressed in intercalated cells (Yang et al., 2006a), whereas mPGES1 has been detected in principal cells (Chen et al., 2017; Wang et al., 2018; Ransick et al., 2019). The $mCCD_{cl1}$ cell line used in this study is a clonal cell line derived from microdissected mouse CCD and retains features typical for CCD principal cells (Gaeggeler et al., 2005, 2011; Gonzalez-Rodriguez et al., 2007; Mansley et al., 2015, 2018, 2019). Thus, at first sight it may appear surprising that transcripts for mPGES2 but not for mPGES1 were detected in $mCCD_{cl1}$ cells. However, mPGES1 expression is induced by cytokines and inflammatory stimuli (Murakami et al., 2002; Hao and Breyer, 2008). Therefore, basal expression of mPGES1 in CCD principal cells is probably low and may have been below the detection limit in $mCCD_{cl1}$ cells. Low basal expression of mPGES1 is also consistent with the finding that single-cell transcriptome analysis of major renal collecting duct cells types in mouse revealed a weaker expression of mPGES1 in CCD principal cells compared with cPGES (Chen et al., 2017). Interestingly, it has been reported that $mCCD_{cl1}$ cells show some plasticity consistent with the ability to transition between principal and intercalated cells (Assmus et al., 2018). There is little doubt that the ENaC-dependent I_{SC} observed in the present study is generated by $mCCD_{cl1}$ cells that predominantly behave like principal cells. However, at present it is unclear whether PGE_2 synthesis and

secretion occurs in the same cells responsible for the amiloride-sensitive I_{SC} or whether this occurs in distinct interspersed cells with an intercalated phenotype that may be present in the $mCCD_{cl1}$ monolayer. It is tempting to speculate that the latter scenario may provide a mechanism by which intercalated cells can regulate principal cell ion transport function in a paracrine manner. Whether this occurs in native tissue and is physiologically relevant remains to be determined.

The biotinylation experiments performed in this study indicate that PGE_2 stimulates ENaC activity at least in part by increasing the abundance of ENaC at the apical plasma membrane. This is consistent with the finding that PGE_2 via EP_4 receptor increases cytosolic cAMP in $mCCD_{cl1}$ cells, as increased surface abundance of ENaC has previously been observed in response to an elevated cytosolic cAMP concentration (Snyder, 2000; Butterworth et al., 2005). Indeed, it is well known that vasopressin can stimulate ENaC-mediated sodium transport (Schafer and Troutman, 1990; Ecelbarger et al., 2000; Ecelbarger et al., 2001; Nicco et al., 2001) via the $G_{\alpha s}$-coupled V_2-receptor and subsequent activation of the AC/cAMP/PKA pathway (Schafer and Hawk, 1992; Loffing and Korbmacher, 2009; Roos et al., 2013). This involves an increased abundance of the β- and γ-ENaC subunits at the apical plasma membrane, possibly due to the insertion of ENaC-containing vesicles into the plasma membrane from a subapical pool (Snyder, 2000; Butterworth et al., 2005, 2012). Additional mechanisms probably contribute to stimulate ENaC activity following the activation of the AC/cAMP/PKA pathway (e.g., phosphorylation events; Yang et al., 2006b) and an increase in channel open probability (Bugaj et al., 2009). Thus, the stimulatory effect of PGE_2 on ENaC, like that of vasopressin, is probably more complex than simply increasing channel surface expression (Kortenoeven et al., 2015).

The conclusion that the PGE_2 effect on ENaC is mediated by an activation of the AC/cAMP/PKA pathway is further supported by the observation that the effects of PGE_2 and vasopressin were nonadditive in $mCCD_{cl1}$ cells. This indicates that the signaling pathways of PGE_2 and vasopressin converge. Importantly, the stimulatory effect of PGE_2 on ENaC activity was preserved when $mCCD_{cl1}$ cells were prestimulated with aldosterone. In contrast to the rapid effects of PGE_2 and vasopressin, the stimulatory effect of aldosterone was much slower. This slower time course of the aldosterone response is consistent with observations in isolated perfused rat CCD (Reif et al., 1986). It is not surprising, because the response to aldosterone is mediated by the mineralocorticoid receptor and involves highly complex regulatory mechanisms that are not yet fully understood but include transcriptional regulation of the channel and of regulatory proteins (Loffing and Korbmacher, 2009; Rossier, 2014).

It has been postulated that the well-documented synergistic stimulation of sodium transport by vasopressin and aldosterone (Tomita et al., 1985; Reif et al., 1986; Chen et al., 1990, 1991; Schafer and Hawk, 1992; Snyder et al., 2004; Bugaj et al., 2009) is important to achieve maximal sodium reabsorption and urine concentration due to the simultaneous stimulation of water permeability by vasopressin (Reif et al., 1986). At present, the role of PGE_2 in regulating sodium and water transport in the distal nephron and collecting duct is less clear. It is commonly thought that prostanoids synthesized along the renal tubular system cause natriuresis by reducing medullary sodium and water reabsorption. This may be particularly relevant under conditions of elevated salt intake (Hao and Breyer, 2007) or when tubular fluid flow is high (Flores et al., 2012). Inhibition of sodium and water reabsorption by prostanoids may be due to various mechanisms such as their ability to blunt the action of vasopressin, promote medullary blood flow, and directly inhibit sodium transport in the distal nephron by reducing the activity of the Na^+/K^+-ATPase or ENaC (Stokes and Kokko, 1977; Hébert et al., 1990; Zeidel, 1993; Guan et al., 1998; Hao and Breyer, 2007; Flores et al., 2012). On the other hand, PGE_2 increased water flux and elevated sodium absorption in primary cultures of freshly isolated tubules (Canessa and Schafer, 1992; Wang et al., 2016). Interestingly, the expression pattern of enzymes and receptors associated with prostanoid signaling may be altered under conditions of low salt intake or volume contraction (Hao and Breyer, 2008; Li et al., 2017; Wang et al., 2018). For example, in rabbits, salt restriction markedly stimulated PGE_2 biosynthesis in the outer medulla and cortex (Davila et al., 1978; Stahl et al., 1979). This may indicate that PGE_2 is needed to minimize renal sodium excretion. Thus, there is evidence that the effect of PGE_2 on transepithelial sodium and water flux depends on the physiological or pathophysiologic setting. A different responsiveness to prostanoids may also explain why indomethacin decreased blood pressure in animals on a low-sodium diet but increased blood pressure in sodium-repleted rats (Stahl et al., 1981).

In conclusion, our results demonstrate that PGE_2 can stimulate ENaC in $mCCD_{cl1}$ cells, which depends on EP_4 receptor activation and a rise in cytosolic cAMP. Furthermore, these cells can synthesize and secrete PGE_2, which acts in an autocrine/paracrine manner to stimulate ENaC-mediated sodium transport. The (patho-)physiological implications of these findings remain to be elucidated. However, the findings suggest that under certain conditions, locally generated PGE_2 may stimulate sodium absorption in the ASDN. Conversely, it is conceivable that pharmacological inhibition of PGE_2 synthesis may attenuate sodium reabsorption in the ASDN in states with increased local production of PGE_2. Additional studies are needed in native tissue and genetically modified animal models to explore a possible dual regulatory role of PGE_2 associated with its ability to inhibit or stimulate sodium absorption in collecting duct cells.

Acknowledgments

David A. Eisner served as editor.

Part of the present work was performed in fulfilment of the requirements for obtaining the degree "Dr. med." (C. Niklas) and "Dr. rer. nat." (R. Nacken), and was published in abstract form (Niklas et al. 2011 Acta Physiol 201 [Suppl 682]: P101; Niklas et al. 2010, Acta Physiol 201 [Suppl 677]: O-TUE-3-6).

The technical assistance of Lorenz Reeh and Jessica Rinke is gratefully acknowledged.

This study was supported by the Deutsche Forschungsgemeinschaft (DFG, German Research Foundation), project number 387509280, SFB

1350), the Alexander von Humboldt Foundation (3.3-GRO/1143730 STP), the Interdisziplinäres Zentrum für Klinische Forschung of Friedrich-Alexander University (IZKF, TP-A33), and the Bayerische Forschungsstiftung (PDOK-74-10).

The authors declare no competing financial interests.

Author contributions: C. Korbmacher and M. Bertog contributed to conception of research; M.K. Mansley, C. Niklas, K. Mandery, R. Nacken, H. Glaeser, and M. Bertog performed experiments and analyzed data; M.K. Mansley, C. Niklas, M. Fromm, C. Korbmacher, and M. Bertog interpreted results of experiments; M.K. Mansley and M. Bertog prepared figures; M.K. Mansley, C. Korbmacher and M. Bertog drafted and edited manuscript; and all authors approved final version of the manuscript.

Submitted: 2 November 2019
Revised: 30 March 2020
Accepted: 21 April 2020

References

Arakawa, T., O. Laneuville, C.A. Miller, K.M. Lakkides, B.A. Wingerd, D.L. DeWitt, and W.L. Smith. 1996. Prostanoid receptors of murine NIH 3T3 and RAW 264.7 cells. Structure and expression of the murine prostaglandin EP4 receptor gene. *J. Biol. Chem.* 271:29569–29575. https://doi.org/10.1074/jbc.271.47.29569

Assmus, A.M., M.K. Mansley, L.J. Mullins, A. Peter, and J.J. Mullins. 2018. $mCCD_{cl1}$ cells show plasticity consistent with the ability to transition between principal and intercalated cells. *Am. J. Physiol. Renal Physiol.* 314:F820–F831. https://doi.org/10.1152/ajprenal.00354.2017

Bankir, L., D.G. Bichet, and N. Bouby. 2010. Vasopressin V2 receptors, ENaC, and sodium reabsorption: a risk factor for hypertension? *Am. J. Physiol. Renal Physiol.* 299:F917–F928. https://doi.org/10.1152/ajprenal.00413.2010

Bertog, M., B. Letz, W. Kong, M. Steinhoff, M.A. Higgins, A. Bielfeld-Ackermann, E. Frömter, N.W. Bunnett, and C. Korbmacher. 1999. Basolateral proteinase-activated receptor (PAR-2) induces chloride secretion in M-1 mouse renal cortical collecting duct cells. *J. Physiol.* 521:3–17. https://doi.org/10.1111/j.1469-7793.1999.00003.x

Bertog, M., J.E. Cuffe, S. Pradervand, E. Hummler, A. Hartner, M. Porst, K.F. Hilgers, B.C. Rossier, and C. Korbmacher. 2008. Aldosterone responsiveness of the epithelial sodium channel (ENaC) in colon is increased in a mouse model for Liddle's syndrome. *J. Physiol.* 586:459–475. https://doi.org/10.1113/jphysiol.2007.140459

Blanco, G., and D.P. Wallace. 2013. Novel role of ouabain as a cystogenic factor in autosomal dominant polycystic kidney disease. *Am. J. Physiol. Renal Physiol.* 305:F797–F812. https://doi.org/10.1152/ajprenal.00248.2013

Bonvalet, J.P., P. Pradelles, and N. Farman. 1987. Segmental synthesis and actions of prostaglandins along the nephron. *Am. J. Physiol.* 253:F377–F387.

Breyer, M.D., and R.M. Breyer. 2000a. Prostaglandin E receptors and the kidney. *Am. J. Physiol. Renal Physiol.* 279:F12–F23. https://doi.org/10.1152/ajprenal.2000.279.1.F12

Breyer, M.D., and R.M. Breyer. 2000b. Prostaglandin receptors: their role in regulating renal function. *Curr. Opin. Nephrol. Hypertens.* 9:23–29. https://doi.org/10.1097/00041552-200001000-00005

Breyer, M.D., and R.M. Breyer. 2001. G protein-coupled prostanoid receptors and the kidney. *Annu. Rev. Physiol.* 63:579–605. https://doi.org/10.1146/annurev.physiol.63.1.579

Bugaj, V., O. Pochynyuk, and J.D. Stockand. 2009. Activation of the epithelial Na+ channel in the collecting duct by vasopressin contributes to water reabsorption. *Am. J. Physiol. Renal Physiol.* 297:F1411–F1418. https://doi.org/10.1152/ajprenal.00371.2009

Butterworth, M.B., R.S. Edinger, J.P. Johnson, and R.A. Frizzell. 2005. Acute ENaC stimulation by cAMP in a kidney cell line is mediated by exocytic insertion from a recycling channel pool. *J. Gen. Physiol.* 125:81–101. https://doi.org/10.1085/jgp.200409124

Butterworth, M.B., R.S. Edinger, M.R. Silvis, L.I. Gallo, X. Liang, G. Apodaca, R.A. Frizzell, and J.P. Johnson. 2012. Rab11b regulates the trafficking and recycling of the epithelial sodium channel (ENaC). *Am. J. Physiol. Renal Physiol.* 302:F581–F590. https://doi.org/10.1152/ajprenal.00304.2011

Câmpean, V., F. Theilig, A. Paliege, M. Breyer, and S. Bachmann. 2003. Key enzymes for renal prostaglandin synthesis: site-specific expression in rodent kidney (rat, mouse). *Am. J. Physiol. Renal Physiol.* 285:F19–F32. https://doi.org/10.1152/ajprenal.00443.2002

Canessa, C.M., and J.A. Schafer. 1992. AVP stimulates Na+ transport in primary cultures of rabbit cortical collecting duct cells. *Am. J. Physiol.* 262:F454–F461.

Chen, L., S.K. Williams, and J.A. Schafer. 1990. Differences in synergistic actions of vasopressin and deoxycorticosterone in rat and rabbit CCD. *Am. J. Physiol.* 259:F147–F156.

Chen, L., M.C. Reif, and J.A. Schafer. 1991. Clonidine and PGE2 have different effects on Na+ and water transport in rat and rabbit CCD. *Am. J. Physiol.* 261:F126–F136.

Chen, L., J.W. Lee, C.L. Chou, A.V. Nair, M.A. Battistone, T.G. Păunescu, M. Merkulova, S. Breton, J.W. Verlander, S.M. Wall, et al. 2017. Transcriptomes of major renal collecting duct cell types in mouse identified by single-cell RNA-seq. *Proc. Natl. Acad. Sci. USA.* 114:E9989–E9998. https://doi.org/10.1073/pnas.1710964114

Davila, D., T. Davila, E. Oliw, and E. Anggård. 1978. The influence of dietary sodium on urinary prostaglandin excretion. *Acta Physiol. Scand.* 103:100–106. https://doi.org/10.1111/j.1748-1716.1978.tb06195.x

Ecelbarger, C.A., G.H. Kim, J. Terris, S. Masilamani, C. Mitchell, I. Reyes, J.G. Verbalis, and M.A. Knepper. 2000. Vasopressin-mediated regulation of epithelial sodium channel abundance in rat kidney. *Am. J. Physiol. Renal Physiol.* 279:F46–F53. https://doi.org/10.1152/ajprenal.2000.279.1.F46

Ecelbarger, C.A., G.H. Kim, J.B. Wade, and M.A. Knepper. 2001. Regulation of the abundance of renal sodium transporters and channels by vasopressin. *Exp. Neurol.* 171:227–234. https://doi.org/10.1006/exnr.2001.7775

Edinger, R.S., C. Coronnello, A.J. Bodnar, M. Labarca, V. Bhalla, W.A. La-Framboise, P.V. Benos, J. Ho, J.P. Johnson, and M.B. Butterworth. 2014. Aldosterone regulates microRNAs in the cortical collecting duct to alter sodium transport. *J. Am. Soc. Nephrol.* 25:2445–2457. https://doi.org/10.1681/ASN.2013090931

Fenton, R.A., and M.A. Knepper. 2007. Mouse models and the urinary concentrating mechanism in the new millennium. *Physiol. Rev.* 87:1083–1112. https://doi.org/10.1152/physrev.00053.2006

Flores, D., Y. Liu, W. Liu, L.M. Satlin, and R. Rohatgi. 2012. Flow-induced prostaglandin E2 release regulates Na and K transport in the collecting duct. *Am. J. Physiol. Renal Physiol.* 303:F632–F638. https://doi.org/10.1152/ajprenal.00169.2012

Fujino, H., and J.W. Regan. 2006. EP(4) prostanoid receptor coupling to a pertussis toxin-sensitive inhibitory G protein. *Mol. Pharmacol.* 69:5–10. https://doi.org/10.1124/mol.105.017749

Gaeggeler, H.P., E. Gonzalez-Rodriguez, N.F. Jaeger, D. Loffing-Cueni, R. Norregaard, J. Loffing, J.D. Horisberger, and B.C. Rossier. 2005. Mineralocorticoid versus glucocorticoid receptor occupancy mediating aldosterone-stimulated sodium transport in a novel renal cell line. *J. Am. Soc. Nephrol.* 16:878–891. https://doi.org/10.1681/ASN.2004121110

Gaeggeler, H.P., Y. Guillod, D. Loffing-Cueni, J. Loffing, and B.C. Rossier. 2011. Vasopressin-dependent coupling between sodium transport and water flow in a mouse cortical collecting duct cell line. *Kidney Int.* 79:843–852. https://doi.org/10.1038/ki.2010.486

Gao, M., R. Cao, S. Du, X. Jia, S. Zheng, S. Huang, Q. Han, J. Liu, X. Zhang, Y. Miao, et al. 2015. Disruption of prostaglandin E2 receptor EP4 impairs urinary concentration via decreasing aquaporin 2 in renal collecting ducts. *Proc. Natl. Acad. Sci. USA.* 112:8397–8402. https://doi.org/10.1073/pnas.1509565112

Garty, H., and L.G. Palmer. 1997. Epithelial sodium channels: function, structure, and regulation. *Physiol. Rev.* 77:359–396. https://doi.org/10.1152/physrev.1997.77.2.359

Gonzalez-Rodriguez, E., H.P. Gaeggeler, and B.C. Rossier. 2007. IGF-1 vs insulin: respective roles in modulating sodium transport via the PI-3 kinase/Sgk1 pathway in a cortical collecting duct cell line. *Kidney Int.* 71:116–125. https://doi.org/10.1038/sj.ki.5002018

Grantham, J.J., and J. Orloff. 1968. Effect of prostaglandin E1 on the permeability response of the isolated collecting tubule to vasopressin, adenosine 3′,5′-monophosphate, and theophylline. *J. Clin. Invest.* 47:1154–1161. https://doi.org/10.1172/JCI105804

Guan, Y., Y. Zhang, R.M. Breyer, B. Fowler, L. Davis, R.L. Hébert, and M.D. Breyer. 1998. Prostaglandin E2 inhibits renal collecting duct Na+

absorption by activating the EP1 receptor. *J. Clin. Invest.* 102:194–201. https://doi.org/10.1172/JCI2872

Hao, C.M., and M.D. Breyer. 2007. Physiologic and pathophysiologic roles of lipid mediators in the kidney. *Kidney Int.* 71:1105–1115. https://doi.org/10.1038/sj.ki.5002192

Hao, C.M., and M.D. Breyer. 2008. Physiological regulation of prostaglandins in the kidney. *Annu. Rev. Physiol.* 70:357–377. https://doi.org/10.1146/annurev.physiol.70.113006.100614

Hébert, R.L., H.R. Jacobson, and M.D. Breyer. 1990. PGE2 inhibits AVP-induced water flow in cortical collecting ducts by protein kinase C activation. *Am. J. Physiol.* 259:F318–F325.

Hébert, R.L., H.R. Jacobson, and M.D. Breyer. 1991. Prostaglandin E2 inhibits sodium transport in rabbit cortical collecting duct by increasing intracellular calcium. *J. Clin. Invest.* 87:1992–1998. https://doi.org/10.1172/JCI115227

Iino, Y., and M. Imai. 1978. Effects of prostaglandins on Na transport in isolated collecting tubules. *Pflugers Arch.* 373:125–132. https://doi.org/10.1007/BF00584850

Jensen, B.L., J. Stubbe, P.B. Hansen, D. Andreasen, and O. Skøtt. 2001. Localization of prostaglandin E(2) EP2 and EP4 receptors in the rat kidney. *Am. J. Physiol. Renal Physiol.* 280:F1001–F1009. https://doi.org/10.1152/ajprenal.2001.280.6.F1001

Kiriyama, M., F. Ushikubi, T. Kobayashi, M. Hirata, Y. Sugimoto, and S. Narumiya. 1997. Ligand binding specificities of the eight types and subtypes of the mouse prostanoid receptors expressed in Chinese hamster ovary cells. *Br. J. Pharmacol.* 122:217–224. https://doi.org/10.1038/sj.bjp.0701367

Kirschenbaum, M.A., and J.H. Stein. 1976. The effect of inhibition of prostaglandin synthesis on urinary sodium excretion in the conscious dog. *J. Clin. Invest.* 57:517–521. https://doi.org/10.1172/JCI108304

Kleyman, T.R., O.B. Kashlan, and R.P. Hughey. 2018. Epithelial Na^+ Channel Regulation by Extracellular and Intracellular Factors. *Annu. Rev. Physiol.* 80:263–281. https://doi.org/10.1146/annurev-physiol-021317-121143

Kokko, K.E., P.S. Matsumoto, B.N. Ling, and D.C. Eaton. 1994. Effects of prostaglandin E2 on amiloride-blockable Na+ channels in a distal nephron cell line (A6). *Am. J. Physiol.* 267:C1414–C1425. https://doi.org/10.1152/ajpcell.1994.267.5.C1414

Kokko, K.E., P.S. Matsumoto, Z.R. Zhang, B.N. Ling, and D.C. Eaton. 1997. Prostaglandin E2 increases 7-pS Cl- channel density in the apical membrane of A6 distal nephron cells. *Am. J. Physiol.* 273:C548–C557. https://doi.org/10.1152/ajpcell.1997.273.2.C548

Kortenoeven, M.L., N.B. Pedersen, L.L. Rosenbaek, and R.A. Fenton. 2015. Vasopressin regulation of sodium transport in the distal nephron and collecting duct. *Am. J. Physiol. Renal Physiol.* 309:F280–F299. https://doi.org/10.1152/ajprenal.00093.2015

Krueger, B., S. Haerteis, L. Yang, A. Hartner, R. Rauh, C. Korbmacher, and A. Diakov. 2009. Cholesterol depletion of the plasma membrane prevents activation of the epithelial sodium channel (ENaC) by SGK1. *Cell. Physiol. Biochem.* 24:605–618. https://doi.org/10.1159/000257516

Li, J.H., C.L. Chou, B. Li, O. Gavrilova, C. Eisner, J. Schnermann, S.A. Anderson, C.X. Deng, M.A. Knepper, and J. Wess. 2009. A selective EP4 PGE2 receptor agonist alleviates disease in a new mouse model of X-linked nephrogenic diabetes insipidus. *J. Clin. Invest.* 119:3115–3126. https://doi.org/10.1172/JCI39680

Li, Y., Y. Wei, F. Zheng, Y. Guan, and X. Zhang. 2017. Prostaglandin E2 in the Regulation of Water Transport in Renal Collecting Ducts. *Int. J. Mol. Sci.* 18:2539. https://doi.org/10.3390/ijms18122539

Ling, B.N., K.E. Kokko, and D.C. Eaton. 1992. Inhibition of apical Na+ channels in rabbit cortical collecting tubules by basolateral prostaglandin E2 is modulated by protein kinase C. *J. Clin. Invest.* 90:1328–1334. https://doi.org/10.1172/JCI115998

Liu, Y., M. Rajagopal, K. Lee, L. Battini, D. Flores, G.L. Gusella, A.C. Pao, and R. Rohatgi. 2012. Prostaglandin E(2) mediates proliferation and chloride secretion in ADPKD cystic renal epithelia. *Am. J. Physiol. Renal Physiol.* 303:F1425–F1434. https://doi.org/10.1152/ajprenal.00010.2012

Liu, Y., D. Flores, R. Carrisoza-Gaytán, and R. Rohatgi. 2014. Biomechanical regulation of cyclooxygenase-2 in the renal collecting duct. *Am. J. Physiol. Renal Physiol.* 306:F214–F223. https://doi.org/10.1152/ajprenal.00327.2013

Loffing, J., and C. Korbmacher. 2009. Regulated sodium transport in the renal connecting tubule (CNT) via the epithelial sodium channel (ENaC). *Pflugers Arch.* 458:111–135. https://doi.org/10.1007/s00424-009-0656-0

Mansley, M.K., W. Neuhuber, C. Korbmacher, and M. Bertog. 2015. Norepinephrine stimulates the epithelial Na+ channel in cortical collecting duct cells via α2-adrenoceptors. *Am. J. Physiol. Renal Physiol.* 308:F450–F458. https://doi.org/10.1152/ajprenal.00548.2014

Mansley, M.K., C. Korbmacher, and M. Bertog. 2018. Inhibitors of the proteasome stimulate the epithelial sodium channel (ENaC) through SGK1 and mimic the effect of aldosterone. *Pflugers Arch.* 470:295–304. https://doi.org/10.1007/s00424-017-2060-5

Mansley, M.K., A.J. Roe, S.L. Francis, J.H. Gill, M.A. Bailey, and S.M. Wilson. 2019. Trichostatin A blocks aldosterone-induced Na^+ transport and control of serum- and glucocorticoid-inducible kinase 1 in cortical collecting duct cells. *Br. J. Pharmacol.* 176:4708–4719. https://doi.org/10.1111/bph.14837

Matsumoto, P.S., L. Mo, and N.K. Wills. 1997. Osmotic regulation of Na+ transport across A6 epithelium: interactions with prostaglandin E2 and cyclic AMP. *J. Membr. Biol.* 160:27–38. https://doi.org/10.1007/s002329900292

Murakami, M., Y. Nakatani, T. Tanioka, and I. Kudo. 2002. Prostaglandin E synthase. *Prostaglandins Other Lipid Mediat.* 68–69:383–399. https://doi.org/10.1016/S0090-6980(02)00043-6

Narumiya, S., Y. Sugimoto, and F. Ushikubi. 1999. Prostanoid receptors: structures, properties, and functions. *Physiol. Rev.* 79:1193–1226. https://doi.org/10.1152/physrev.1999.79.4.1193

Nasrallah, R., J. Zimpelmann, D. Eckert, J. Ghossein, S. Geddes, J.C. Beique, J.F. Thibodeau, C.R.J. Kennedy, K.D. Burns, and R.L. Hébert. 2018. PGE_2 EP_1 receptor inhibits vasopressin-dependent water reabsorption and sodium transport in mouse collecting duct. *Lab. Invest.* 98:360–370. https://doi.org/10.1038/labinvest.2017.133

Nesterov, V., B. Krueger, M. Bertog, A. Dahlmann, R. Palmisano, and C. Korbmacher. 2016. In Liddle Syndrome, Epithelial Sodium Channel Is Hyperactive Mainly in the Early Part of the Aldosterone-Sensitive Distal Nephron. *Hypertension.* 67:1256–1262. https://doi.org/10.1161/HYPERTENSIONAHA.115.07061

Nicco, C., M. Wittner, A. DiStefano, S. Jounier, L. Bankir, and N. Bouby. 2001. Chronic exposure to vasopressin upregulates ENaC and sodium transport in the rat renal collecting duct and lung. *Hypertension.* 38:1143–1149. https://doi.org/10.1161/hy1001.092641

Olesen, E.T., M.R. Rützler, H.B. Moeller, H.A. Praetorius, and R.A. Fenton. 2011. Vasopressin-independent targeting of aquaporin-2 by selective E-prostanoid receptor agonists alleviates nephrogenic diabetes insipidus. *Proc. Natl. Acad. Sci. USA.* 108:12949–12954. https://doi.org/10.1073/pnas.1104691108

Olesen, E.T., H.B. Moeller, M. Assentoft, N. MacAulay, and R.A. Fenton. 2016. The vasopressin type 2 receptor and prostaglandin receptors EP2 and EP4 can increase aquaporin-2 plasma membrane targeting through a cAMP-independent pathway. *Am. J. Physiol. Renal Physiol.* 311:F935–F944. https://doi.org/10.1152/ajprenal.00559.2015

Pavlov, T.S., D.V. Ilatovskaya, V. Levchenko, D.L. Mattson, R.J. Roman, and A. Staruschenko. 2011. Effects of cytochrome P-450 metabolites of arachidonic acid on the epithelial sodium channel (ENaC). *Am. J. Physiol. Renal Physiol.* 301:F672–F681. https://doi.org/10.1152/ajprenal.00597.2010

Rajagopal, M., S.V. Thomas, P.P. Kathpalia, Y. Chen, and A.C. Pao. 2014. Prostaglandin E2 induces chloride secretion through crosstalk between cAMP and calcium signaling in mouse inner medullary collecting duct cells. *Am. J. Physiol. Cell Physiol.* 306:C263–C278. https://doi.org/10.1152/ajpcell.00381.2012

Ransick, A., N.O. Lindström, J. Liu, Q. Zhu, J.-J. Guo, G.F. Alvarado, A.D. Kim, H.G. Black, J. Kim, and A.P. McMahon. 2019. Single-Cell Profiling Reveals Sex, Lineage, and Regional Diversity in the Mouse Kidney. *Dev. Cell.* 51:399–413.e7. https://doi.org/10.1016/j.devcel.2019.10.005

Reif, M.C., S.L. Troutman, and J.A. Schafer. 1986. Sodium transport by rat cortical collecting tubule. Effects of vasopressin and desoxycorticosterone. *J. Clin. Invest.* 77:1291–1298. https://doi.org/10.1172/JCI112433

Roos, K.P., V. Bugaj, E. Mironova, J.D. Stockand, N. Ramkumar, S. Rees, and D.E. Kohan. 2013. Adenylyl cyclase VI mediates vasopressin-stimulated ENaC activity. *J. Am. Soc. Nephrol.* 24:218–227. https://doi.org/10.1681/ASN.2012050449

Rossier, B.C.. 2014. Epithelial sodium channel (ENaC) and the control of blood pressure. *Curr. Opin. Pharmacol.* 15:33–46. https://doi.org/10.1016/j.coph.2013.11.010

Sandrasagra, S., J.E. Cuffe, E.L. Regardsoe, and C. Korbmacher. 2004. PGE2 stimulates Cl- secretion in murine M-1 cortical collecting duct cells in an autocrine manner. *Pflugers Arch.* 448:411–421. https://doi.org/10.1007/s00424-004-1260-y

Schafer, J.A., and C.T. Hawk. 1992. Regulation of Na+ channels in the cortical collecting duct by AVP and mineralocorticoids. *Kidney Int.* 41:255–268. https://doi.org/10.1038/ki.1992.37

Schafer, J.A., and S.L. Troutman. 1990. cAMP mediates the increase in apical membrane Na+ conductance produced in rat CCD by vasopressin. *Am. J. Physiol.* 259:F823–F831.

Snyder, P.M.. 2000. Liddle's syndrome mutations disrupt cAMP-mediated translocation of the epithelial Na(+) channel to the cell surface. *J. Clin. Invest.* 105:45–53. https://doi.org/10.1172/JCI7869

Snyder, P.M., D.R. Olson, R. Kabra, R. Zhou, and J.C. Steines. 2004. cAMP and serum and glucocorticoid-inducible kinase (SGK) regulate the epithelial Na(+) channel through convergent phosphorylation of Nedd4-2. *J. Biol. Chem.* 279:45753–45758. https://doi.org/10.1074/jbc.M407858200

Soodvilai, S., Z. Jia, M.H. Wang, Z. Dong, and T. Yang. 2009. mPGES-1 deletion impairs diuretic response to acute water loading. *Am. J. Physiol. Renal Physiol.* 296:F1129–F1135. https://doi.org/10.1152/ajprenal.90478.2008

Stahl, R.A., A.A. Attallah, D.L. Bloch, and J.B. Lee. 1979. Stimulation of rabbit renal PGE2 biosynthesis by dietary sodium restriction. *Am. J. Physiol.* 237:F344–F349.

Stahl, R., H. Dienemann, K. Besserer, U. Kneissler, and U. Helmchen. 1981. Effect of indomethacin on blood pressure in rats with renovascular hypertension: dependence on plasma renin activity. *Klin. Wochenschr.* 59:245–246. https://doi.org/10.1007/BF01476582

Stokes, J.B., and J.P. Kokko. 1977. Inhibition of sodium transport by prostaglandin E2 across the isolated, perfused rabbit collecting tubule. *J. Clin. Invest.* 59:1099–1104. https://doi.org/10.1172/JCI108733

Tanikawa, N., Y. Ohmiya, H. Ohkubo, K. Hashimoto, K. Kangawa, M. Kojima, S. Ito, and K. Watanabe. 2002. Identification and characterization of a novel type of membrane-associated prostaglandin E synthase. *Biochem. Biophys. Res. Commun.* 291:884–889. https://doi.org/10.1006/bbrc.2002.6531

Tomita, K., J.J. Pisano, and M.A. Knepper. 1985. Control of sodium and potassium transport in the cortical collecting duct of the rat. Effects of bradykinin, vasopressin, and deoxycorticosterone. *J. Clin. Invest.* 76:132–136. https://doi.org/10.1172/JCI111935

Vitzthum, H., I. Abt, S. Einhellig, and A. Kurtz. 2002. Gene expression of prostanoid forming enzymes along the rat nephron. *Kidney Int.* 62:1570–1581. https://doi.org/10.1046/j.1523-1755.2002.00615.x

Wang, F., X. Lu, K. Peng, H. Fang, L. Zhou, J. Su, A. Nau, K.T. Yang, A. Ichihara, A. Lu, et al. 2016. Antidiuretic Action of Collecting Duct (Pro) Renin Receptor Downstream of Vasopressin and PGE2 Receptor EP4. *J. Am. Soc. Nephrol.* 27:3022–3034. https://doi.org/10.1681/ASN.2015050592

Wang, J., M. Liu, X. Zhang, G. Yang, and L. Chen. 2018. Physiological and pathophysiological implications of PGE_2 and the PGE_2 synthases in the kidney. *Prostaglandins Other Lipid Mediat.* 134:1–6. https://doi.org/10.1016/j.prostaglandins.2017.10.006

Wegmann, M., and R.M. Nüsing. 2003. Prostaglandin E2 stimulates sodium reabsorption in MDCK C7 cells, a renal collecting duct principal cell model. *Prostaglandins Leukot. Essent. Fatty Acids.* 69:315–322. https://doi.org/10.1016/j.plefa.2003.06.002

Wei, Y., D.H. Lin, R. Kemp, G.S. Yaddanapudi, A. Nasjletti, J.R. Falck, and W.H. Wang. 2004. Arachidonic acid inhibits epithelial Na channel via cytochrome P450 (CYP) epoxygenase-dependent metabolic pathways. *J. Gen. Physiol.* 124:719–727. https://doi.org/10.1085/jgp.200409140

Woollhead, A.M., and D.L. Baines. 2006. Forskolin-induced cell shrinkage and apical translocation of functional enhanced green fluorescent protein-human alphaENaC in H441 lung epithelial cell monolayers. *J. Biol. Chem.* 281:5158–5168. https://doi.org/10.1074/jbc.M509947200

Worrell, R.T., H.F. Bao, D.D. Denson, and D.C. Eaton. 2001. Contrasting effects of cPLA2 on epithelial Na+ transport. *Am. J. Physiol. Cell Physiol.* 281:C147–C156. https://doi.org/10.1152/ajpcell.2001.281.1.C147

Yang, T., I. Singh, H. Pham, D. Sun, A. Smart, J.B. Schnermann, and J.P. Briggs. 1998. Regulation of cyclooxygenase expression in the kidney by dietary salt intake. *Am. J. Physiol.* 274:F481–F489.

Yang, G., L. Chen, Y. Zhang, X. Zhang, J. Wu, S. Li, M. Wei, Z. Zhang, M.D. Breyer, and Y. Guan. 2006a. Expression of mouse membrane-associated prostaglandin E2 synthase-2 (mPGES-2) along the urogenital tract. *Biochim. Biophys. Acta.* 1761:1459–1468. https://doi.org/10.1016/j.bbalip.2006.06.018

Yang, L.M., R. Rinke, and C. Korbmacher. 2006b. Stimulation of the epithelial sodium channel (ENaC) by cAMP involves putative ERK phosphorylation sites in the C termini of the channel's beta- and gamma-subunit. *J. Biol. Chem.* 281:9859–9868. https://doi.org/10.1074/jbc.M512046200

Zeidel, M.L.. 1993. Hormonal regulation of inner medullary collecting duct sodium transport. *Am. J. Physiol.* 265:F159–F173.

Zhang, Y., A. Schneider, R. Rao, W.J. Lu, X. Fan, L. Davis, R.M. Breyer, M.D. Breyer, and Y. Guan. 2003. Genomic structure and genitourinary expression of mouse cytosolic prostaglandin E(2) synthase gene. *Biochim. Biophys. Acta.* 1634:15–23. https://doi.org/10.1016/j.bbalip.2003.08.003